

# Geology of the Guaje Mountain 7.5-minute quadrangle, Los Alamos and Sandoval Counties, New Mexico

Kirt Kempter<sup>1</sup>, Shari Kelley<sup>2</sup>, Jamie Gardner<sup>3</sup>, Steve Reneau<sup>3</sup>, David Broxton<sup>3</sup>,  
Fraser Goff<sup>3</sup>, Alexis Lavine<sup>3</sup>, Claudia Lewis<sup>3</sup>

1. 2623 Via Caballero del Norte, Santa Fe, NM, 87505
2. New Mexico Bureau of Geology and Mineral Resources, New Mexico Tech, Socorro, NM 87801
3. Earth and Environmental Science Division, Los Alamos National Laboratory, Los Alamos, NM 87545



New Mexico Bureau of Geology and Mineral Resource, Open-file Geologic Map OF-GM 55  
May, 2002  
Updated September, 2004 and June, 2007

## **Location**

The Guaje Mountain quadrangle straddles the boundary between the eastern Jemez Mountains and the Pajarito Plateau. East-dipping mesas and east to southeasterly-trending steep-sided canyons characterize the Pajarito Plateau. The Jemez Mountains are predominantly formed by the 18.7 Ma to ~50 ka Jemez volcanic field. Volcanic activity in the Jemez Mountains culminated with the formation of two geographically coincident calderas, the 1.61 Ma Toledo caldera and 1.25 Ma Valles caldera, both of which lie to the west of the quadrangle. This area is in the western part of the Española Basin, one of several basins in the northerly-trending Rio Grande rift; the western margin of the Española Basin is under the western part of the volcanic pile. The town of Los Alamos occupies the southern fourth of the area. The main facilities associated with Los Alamos National Laboratory are located along the southern edge of the quadrangle. The Santa Clara Indian Reservation lies in the northern fourth of the quadrangle.

## **Previous Work**

As a consequence of the area's proximity to one of the country's premier scientific institutions (with an unfortunate legacy of haphazard radioactive waste disposal in the 1940s and 1950s), the geology of the Guaje Mountain quadrangle, particularly near the town of Los Alamos, has received considerable attention. A voluminous literature about the hydrology (e.g., Broxton and Vaniman, 2005, and references therein), seismic hazards (e.g., Gardner et al., 1998, 1999, 2001, 2003; Reneau et al. 2002; Lewis et al. 2002; Lavine et al., 2003) and stratigraphy (e.g., Griggs, 19964, Bailey et al. 1969, Smith et al., 1970; WoldeGabriel et al., 2001, 2006; Broxton et al., 2007) is available for the Pajarito Plateau.

The first geologic map of the Guaje Mountain quadrangle was included as part of the map of the Los Alamos area by Griggs (1964). Griggs (1964) and Bailey et al. (1969) described and defined the stratigraphy of the eastern Jemez Mountains. A more detailed map of the area appears on the classic geologic map of the Jemez Mountains by Smith et al. (1970). Part of the quadrangle is on the map of Rogers (1995). Most recently, one of the co-authors, Jamie Gardner, mapped most of the Guaje Mountain quadrangle in his

spare time during the 1990s, but his field maps and notebooks were lost when his home burned during the 2000 Cerro Grande fire. We all appreciate Jamie Gardner's contributions to the current mapping effort.

## **Geologic Overview**

The Guaje Mountain quadrangle contains some of the most spectacular volcanic geology in the state, including exposures of voluminous lava flows and ignimbrite deposits, thick sequences of volcanoclastic sediments, and a linked set of faults related to the Pajarito fault zone. From west to east, rocks in the quadrangle record the geographic transition from pre-caldera Tschicoma Formation on the rim of the Valles caldera to gently-dipping Bandelier Tuff deposits on the Pajarito Plateau to rift-fill fanglomerates of the Puye Formation. Exposures in the region were enhanced by the Cerro Grande fire, which burned across approximately 35% of the area within the quadrangle in May of 2000.

Sporadic outcrops of middle Miocene age basalt of the Lobato Formation, which yields ages of 10.2 to 13.1 Ma, and andesites and trachyandesites of the Paliza Canyon (?) Formation, dated at ~7.8-11.2 Ma (Broxton and Vaniman, 2005; WoldeGabriel et al., 2006; this report), represent the oldest rock units exposed in the map area. These early Jemez volcanic field rocks were likely derived from eruptive centers located northwest and west of the quadrangle. In late Miocene to early Pliocene time, at least four voluminous silicic lavas were emplaced in the quadrangle, forming a dome complex with high-aspect ratio lavas belonging to the Tschicoma Formation (Bailey et al., 1969; Gardner et al., 1986). These porphyritic dacitic to rhyolitic lavas form the present day Sierra de las Valles, which is the eastern topographic rim of the Valles caldera. In response to the emplacement of these voluminous lavas, an eastward-prograding fanglomerate developed, consisting primarily of fluvially-transported Tschicoma Formation dacite and rhyodacite clasts. These fanglomerate deposits, locally intercalated with tephra and small-volume pyroclastic flows, define the Puye Formation (Bailey et al., 1969; Turbeville et al., 1989), with an age range of 5.3 to 2.4 Ma (WoldeGabriel et al., 2001). Reneau and McDonald (1996) note that, as defined by Griggs (1964) and Bailey et al., 1969), the Puye Formation is older than the 1.61 Ma Otowi Member of the

Bandelier Tuff; however, Puye-like gravels are in Cerro Toledo deposits above the Otowi Member. Furthermore, these gravels are present on the 1.25 Ma Tshirege Member of the Bandelier Tuff, and Puye-like deposition continues in present-day drainages.

Subsequent caldera-forming eruptions of the Bandelier Tuff at 1.61 and 1.25 Ma (WoldeGabriel et al., 2001; Phillips, 2004) filled numerous paleovalleys between and on the Tschicoma Formation lava flows, creating the eastward-dipping Pajarito Plateau surface. A 0.4 m.y. interval of tephra and sedimentary deposition occurred in the region between the two caldera-forming eruptions. These deposits, in part related to silicic eruptions in the vicinity of the Toledo embayment (Stix et al., 1988; Stix, 1989; Gardner and Goff, 1996), are informally classified as the Cerro Toledo interval (Smith et al., 1970; Broxton, 2001). Following the upper Bandelier Tuff eruption, and prior to the incision of modern canyons into the Pajarito Plateau, a brief interval of Quaternary sedimentation occurred upon the Bandelier Tuff, forming alluvial caps on many of the present mesa tops, including several locales in the town of Los Alamos. Other, minor sedimentary units in the map area include landslide, terrace, and recent alluvial deposits.

Faults in the map area cut all of the major stratigraphic units, with the older Tschicoma lavas showing the greatest measurable amount of offset. The largest of these structures, the Pajarito fault zone, has approximately 200 m of cumulative down-to-the east offset of the 1.25 Ma Tshirege Member of the Bandelier Tuff (Gardner et al., 2003). McCalpin (1998) determined that the youngest seismic event on the Pajarito fault occurred 1500 to 2500 years ago, based on analysis of units exposed in seven trenches across the fault just south of Los Alamos Canyon near Camp May Road. Two significant faults strands that have down-to-the-west displacement, the Rendija Canyon fault and the Guaje Mountain fault, are linked to the Pajarito fault and are considered to be part of the Pajarito fault system (Gardner et al. 1999). The Rendija Canyon fault has 40 m and the Guaje Mountain fault has 30 m of maximum vertical displacement (Gardner et al., 2003). Gardner et al. (2003) summarized trench mapping and geochronology data from Chupaderos Canyon, Cabra Canyon, and Rendija Canyon (Wong et al., 1995, Olig et al., 1996, Phillips et al., 1998) to work out the following paleoseismic history of the Guaje Mountain fault:

4000 to 6500 years    1.5 to 2 m of vertical displacement

39,000 years	mainly strike-slip, 0.5 m vertical displacement
40,000 years(?)	1 m vertical displacement in Chupaderos Canyon
144-300 ka	1.5 to 2 m vertical offset here in Rendija Canyon

1.5 to 2 m of displacement in a single seismic event translates to a magnitude 6 to 7 earthquake (Wells and Coppersmith, 1994; Gardner et al., 1999). In the northern portion of the quadrangle structural trends veer to the northwest, parallel to the Santa Clara fault system and the Jemez lineament.

### **Geology from Los Alamos to Santa Clara**

To facilitate interpretation of the area's geologic history, separate discussions are presented for three of the major canyons that drain the quadrangle from west to east. From south to north, these canyons are Los Alamos Canyon, Rendija Canyon, and Guaje Canyon. Exposures in these canyons provide the most complete rock record and interpretive evidence for stratigraphic and structural relationships. An additional discussion is provided for the geology of the Pine Spring area, where many of the quadrangle's major rock units occur within a 1 km<sup>2</sup> area. The deepest canyon on the quadrangle, Santa Clara Canyon, was not accessible because it is on Santa Clara Pueblo land. Map units depicted there are based on air photo and Lidar image interpretations and on the data of Woldegabriel et al. (2006).

A brief list and description of rock units exposed in the Guaje Mountain quadrangle (from oldest to youngest) is supplied below to facilitate the discussion of the geology of each canyon. More detailed and comprehensive unit descriptions are located in the appendix. Age determinations are from WoldeGabriel et al. (2001, 2006), Samuels et al. (2007), and Broxton et al. (2007):

**Lobato Formation basalt** (Miocene, 10.2-13.1 Ma). Small exposures of this unit are in Santa Clara Canyon and in the fault scarp of the Pararito fault zone just north of the Pine Spring area (Smith et al., 1970). These lava flows contain microphenocrysts of plagioclase and olivine.

**Paliza Canyon Formation (?) trachyandesite/ andesite and dacite** (Miocene; 7.8 to 11.2 Ma). Significant exposures are interpreted to be in Santa Clara Canyon and rare outcrops occur in Los Alamos Canyon, Guaje Canyon, and near Pine Springs. The andesitic lava flows contain phenocrysts of plagioclase and clinopyroxene, while the dacite has plagioclase and amphibole phenocrysts.

**Tschicoma Formation (late Miocene to Pliocene).** Silicic, high aspect ratio lava flows that form the topographic highlands along the western portion of the quadrangle. Three units belonging to this episode of volcanism are differentiated: 1) rhyodacite of Rendija Canyon (~5 Ma) - voluminous silicic lavas with plagioclase megacrysts and quartz erupted from a possible vent just west of the west-central quadrangle boundary; 2) dacite of Pajarito Mountain (~3 Ma) - porphyritic dacite lavas erupted from vent(s) at Pajarito Mountain in the SW corner of the quadrangle; 3) dacite of Caballo Mountain (~3 Ma) - porphyritic dacite lavas erupted from vents at/near Caballo Mountain. An unnamed center north of Santa Clara Canyon (Smith et al., 1970) is the likely source for  $3.79 \pm 0.17$  to  $4.39 \pm 0.13$  Ma dacite (WoldeGabriel et al., 2006) exposed in Santa Clara Canyon.

**Puye Formation (late Miocene to Pliocene).** Widely exposed in the eastern half of the quadrangle, these primarily fanglomerate deposits formed as an eastward-prograding alluvial apron from Tschicoma Formation highlands.

**Otowi Member, lower Bandelier Tuff (1.61 Ma).** Erupted from the Toledo caldera, outcrops of this poorly-welded ignimbrite are rare in the quadrangle, restricted to exposures in Rendija, Bayo, and Pueblo canyons in the SE corner of the quadrangle.

**Cerro Toledo deposits (1.61 – 1.25 Ma).** This widespread unit includes all volcanic and sedimentary units deposited between major eruptions of the Bandelier Tuff.

**Tshirege Member, upper Bandelier Tuff (1.25 Ma).** Exposed throughout the quadrangle, this multiple cooling unit ignimbrite defines the Pajarito Plateau and is typically underlain by about 1.5 m of tephra in the Tsankawi Pumice Bed.

**Quaternary old alluvium (<1.25 Ma).** Alluvial sands and gravels cap some of the upper Bandelier Tuff mesas in the quadrangle. These aggradational sediments were deposited prior to the incision of modern canyons across the Pajarito Plateau.

## **Los Alamos Canyon**

Los Alamos Canyon is the deepest canyon in the southern portion of the Guaje Mountain quadrangle and it reveals key stratigraphic relationships, especially for pre-caldera Tschicoma dacite lavas. The canyon makes a gradual bend from south to east above Los Alamos Reservoir. Impressive cliffs of the rhyodacite of Rendija Canyon, locally exceeding 250 m, characterize the upper headwaters of the canyon west of the bend and Quemazon Canyon to the north. The  $4.95 \pm 0.06$  Ma to  $5.32 \pm 0.03$  Ma (Broxton et al., 2007) rhyodacite of Rendija Canyon is composed of multiple flows marked by vesicular flow tops and rubbly, red and black basal breccias. The Los Alamos Canyon area appears to be the southernmost outcrop extent of the Rendija Canyon lavas, which thicken northward towards a possible source vent located just west of the west-central quadrangle boundary. In the vicinity of the bend in Los Alamos Canyon, younger  $2.91 \pm 0.06$  Ma to  $3.07 \pm 0.07$  Ma dacite of Pajarito Mountain (Broxton et al., 2007) overlies the Rendija Canyon lava flows. The overlapping relationship of the Pajarito Mountain flows can be observed on both sides of the canyon just west of the reservoir. On the north canyon wall, two separate Pajarito Mountain lava flows occur, with a pronounced basal breccia at the base of the upper flow and a bed of Puye Formation gravel between the flows.

Subsequently, a large paleovalley was carved in these lavas, roughly coincident with the modern canyon in the bend region. On the south canyon wall by the reservoir a thick sequence (>30 m) of Cerro Toledo deposits is exposed. These deposits consist of primary and reworked tephra and sediments. In general the Cerro Toledo deposits are much thicker on the south side of the canyon, suggesting paleovalley fill prior to the eruption of the upper Bandelier Tuff. Eruption of the upper Bandelier Tuff filled this paleovalley with > 120 m of ignimbrite, now exposed along the southeast wall of the canyon in the bend area. As the canyon bends eastward, Cerro Toledo tephra and sediments overlie the Tschicoma Formation lavas and underlie the upper Bandelier Tuff.

Farther down canyon from the reservoir, the Cerro Toledo deposits are characterized by more fluvial conglomerate facies and less intercalated tephra. The modern Los Alamos Canyon drainage likely developed along the contact of the Cerro Toledo deposits with the Tschicoma Formation lavas (exposed mainly on the north canyon wall).

In the canyon floor immediately east of the reservoir a rare exposure of Miocene andesite crops out beneath the dacite of Pajarito Mountain. This two-pyroxene andesite has been dated at  $8.72 \pm 0.05$  Ma (Broxton and Vaniman, 2005). Chemically, these lavas plot in the middle of the alkalic series of the Keres Group.

Several N-S trending faults related to the Pajarito fault zone cut across the canyon. East of the reservoir, Cerro Toledo deposits are offset by at least 10 meters down-to-the-east, and quickly dip into the subsurface to the east. From this point, outcrops of Bandelier Tuff occur along the valley floor eastward for  $> 3$  km before Cerro Toledo deposits are again exposed on the east side of the down-to-the-west Rendija Fault zone. Los Alamos Canyon represents a shift in Pajarito fault system dynamics, with increasing down-to-the-east displacement south of the canyon and monoclinical folding of the Bandelier Tuff north of the canyon. Most faults north of Los Alamos Canyon, including offsets along the Rendija and Guaje Mountain faults, are down-to-the-west, forming the southern end of the Diamond Drive graben.

Well H-19 (Test Hole 19.6.17.234 of Griggs, 1964) was drilled in Los Alamos Canyon in the vicinity of the Los Alamos skating rink. This 610 m deep well penetrated several dacitic flows (see cross-section B-B'). Broxton et al. (2007) and Samuel et al. (2007) recently dated and geochemically characterized crystal-poor dacite flows encountered in several wells on Los Alamos National Laboratory property south of the Guaje Mountain quadrangle. Samuel et al. (2007) informally name these flows "the northern dacites." Samuel et al. (2007) correlate the northern dacites to the uppermost dacite in H-19. The age of the northern dacites is  $2.47 \pm 0.14$  to  $2.56 \pm 0.06$  Ma, significantly younger than Tschicoma Formation dacites exposed at the surface. The source for these geochemically distinct dacites is unknown, but it is likely in the western Pajarito Plateau (Samuel et al., 2007).

## Rendija Canyon

The steep-sided headwaters of Rendija Canyon are comprised entirely of the rhyodacite of Rendija Canyon. The canyon headwaters were severely affected by the Cerro Grande fire and significant erosion of slope material has occurred. The rhyodacite of Rendija Canyon is porphyritic (see unit descriptions, appendix), containing plagioclase megacrysts (up to 2 cm in diameter), and abundant quartz phenocrysts. Chemically, this lava is a low silica rhyolite (WoldeGabrial, 2001, 2006). In outcrop these lavas characteristically exhibit a rough, knobby surface that weathers to produce angular, gravel-size (1-2 cm) fragments. This weathering phenomenon (possibly related to inherent cooling fractures around plagioclase megacrysts) has been greatly accelerated by heat from the Cerro Grande fire. Post-fire surface spalling of the lavas has produced a huge influx of gravel-size fragments into streams draining Sierra de Los Valles. Thus, aggradation, rather than erosion, characterizes much of the streambed in upper Rendija Canyon.



Fire-induced spalling of Tshirege Member, Bandelier Tuff in Sierra de los Valles.



Flooding events within the first year after the Cerro Grande fire congested several drainages with logs and other fire-related debris.

On the north side Rendija Canyon in northern Los Alamos, continuous exposures of these flows extend eastward from Sierra de Los Valles, forming an irregular-peaked lava ridge to Guaje Mountain. This lava ridge may represent a single flow lobe of Rendija Canyon lava, ponding or piling up to great thickness ( $>100$  meters) in the vicinity of Guaje Mountain. By this interpretation, subsequent down to the west offset along the Rendija and Guaje Mountain faults has produced the present irregular-peaked topography. Alternatively, the lavas may have erupted from separate vents (synchronously) along the Guaje Mountain and Rendija faults, with vents located where topographic peaks adjacent to these faults occur today. There are several examples of vertical flow banding in the lavas along the ridge, especially at Guaje Mountain. However, fieldwork from this study favors a lava flow interpretation, due to: 1) continuity of lava along the east-west ridge, disrupted only by N-S faulting, 2) the lack of field evidence that might suggest overlapping flows from separate vents, and 3) a general continuity of east-dipping topography along the ridge when offsets along the Rendija Canyon and Guaje Mountain faults are restored. A vent just west of the quadrangle

boundary (Gardner et al., 2006) may be the source for the rhyodacite. The lavas were erupted as extremely viscous, high aspect ratio lavas with steep-sided walls that locally collapsed to yield small block and ash flow aprons.



View south across the headwaters of Rendija Canyon from Guaje Ridge toward Pajarito Mountain (note the ski runs). The prominent outcrops are the rhyodacite of Rendija Canyon.

The Otowi Member of the Bandelier Tuff is not preserved in western Rendija Canyon, likely because the Sierra de los Valles highland blocked the emplacement of this tuff. Similarly, Cerro Toldedo deposits are absent in western Rendija Canyon because the ridge of Tschicoma Formation to the north prevented deposition of this unit. Eruption of the Tshirege Member of the Bandelier Tuff filled in many of the paleovalleys carved into the Tschicoma Formation in the Sierra de Los Valles, including the headwaters of Rendija Canyon. In this area, valley ponding of the ignimbrite occurred at varying elevations over relatively short horizontal distances, presumably related to topographic shadow effects of highland topography during ignimbrite emplacement. An example of this topographic variation can be observed north of Rendija Canyon, where ~150 m of elevation difference separates the upper Bandelier Tuff surface over a 0.4 km distance. These variably perched levels of the ignimbrite are clearly related to depositional processes, not faulting. Another common phenomenon observed in the headwaters of Rendija Canyon (and elsewhere in the quadrangle), is lateral drainage migration where streams have formed at the contact between upper Bandelier Tuff and Tschicoma Formation lavas. Incipient streambeds often form at the contact between the upper

Bandelier Tuff and the more resistant Tschicoma Formation lavas. As the softer Bandelier Tuff continually eroded along the contact, the streambed migrates laterally, progressively exhuming the paleotopography of the lava surface.

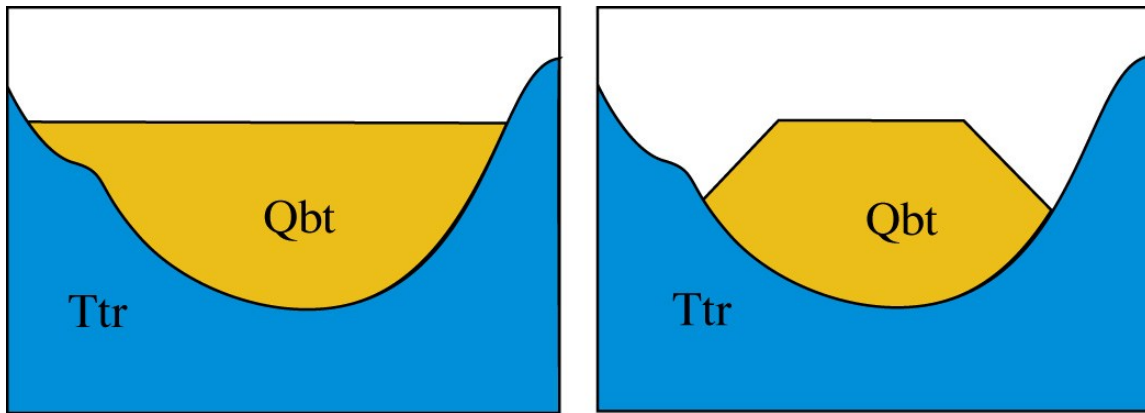


Figure 1. Common drainage evolution observed where Bandelier Tuff has filled in paleovalleys in pre-caldera Tschicoma lavas. Left) Paleovalley fill of Bandelier Tuff. Right) Modern drainages form along contact between Bandelier Tuff and more resistant Tschicoma lavas, progressively exhuming paleoslope of the lavas.

Tshirege Member of the Bandelier Tuff crops out in the canyon and old alluvial deposits rest on the tuff in the middle reaches of Rendija Canyon on the Guaje Mountain quadrangle. The alluvial deposits contain abundant tephra, with subordinate amounts of sand and gravel. The pumice is from Cerro del Medio, which is a dome complex within the Valles caldera built from as many as six eruptions. Phillips (2004) determined a  $^{40}\text{Ar}/^{39}\text{Ar}$  age of  $1.229 \pm 0.017$  Ma from one of the older flows in the complex. The glass in pumice from Cerro del Medio has very distinctive CaO (0.25 – 0.4 wt%) and FeO (0.8 to 1.0 wt %) values compared to pumice from other units, such as the Bandelier Tuff and El Cajete Pumice, on the Pajarito Plateau (Reneau and McDonald, 1996; Reneau et al., 2002). The trace element chemistry of products of the Cerro del Medio eruption is also fairly distinct (150 to 190 ppm Zr, 45 to 55 ppm Nb, 110 to 160 ppm Rb; Spell, 1987; Reneau and McDonald, 1996; Reneau et al., 2002). Pumice sample GMP-04 in Table 1, which was collected from a Qalo deposit exposed in the driveway of the Caballo Peak Apartments on Canyon Drive near the Larry R. Walkup Aquatic Center, has average values of 0.35 wt.% CaO and 0.95 wt % FeO, well within the normal range for Cerro del Medio pumice.

Old alluvium that contains Cerro del Medio pumice underlies much of Western Area and North Community in Los Alamos and covers several mesas south of the town site on Los Alamos National Laboratory property (Reneau et al., 1995, 2002, Gardner et al., 2001; Goff et al., 2001). The early homesteads in the Los Alamos area were sited on mesas capped with old alluvium because water tends to be retained in this unit, a quality that is useful for agriculture. "Beanfield Mesa", a Bandelier Tuff mesa capped by old alluvium that lies between Cabra and Rendija canyons, was farmed in the homestead days of Los Alamos (Martin, 1998). Reneau et al. (1995, 2002) and Gardner et al. (2001) noted that these deposits are remnants of broad early Pleistocene alluvial fans that predate incision of the Pajarito Plateau. Gardner et al. (2001) reported that the gradient on old alluvium is typically less than that of modern streams, roughly paralleling the original top of the Tshirege Member. The old alluvium deposits thin toward the east and are discontinuous.

In the vicinity of Guaje Pines cemetery, the N-S-trending Rendija Canyon fault transects the canyon, uplifting the rhyodacite of Rendija Canyon on the east side of the fault. Offset of the lava along the fault north of the canyon suggests that >100 m of down-to-the-west displacement has occurred. Paleoseismic trenching by Kelson et al. (1996) demonstrates that this fault has repeatedly ruptured during the late Quaternary, with the most recent event at 9 or 23 ka. East of the fault, the canyon narrows where it has carved through the resistant lava, then it widens where younger, softer Cerro Toledo deposits overlie the lava outcrops. The rubbly base of a flow in the rhyodacite is nicely exposed in the northern canyon wall in the narrows. As the valley widens downstream, a flight of seven terrace levels is preserved, probably reflecting strong climatic and depositional variations during the late Quaternary (Reneau et al, 1996). Cerro Toledo deposits are well exposed and occur in thick sequences north of the canyon, including the Cabra Canyon tributary and along the southeastern flank of Guaje Mountain, where >60 m of Cerro Toledo is capped by upper Bandelier Tuff.

East of the Los Alamos Sportsman's Club, small tributary streams on the south side of Rendija Canyon expose rare outcrops of the Otowi Member of the Bandelier Tuff. In general, this unit is more poorly welded than the overlying Tshirege Member and is peppered with small lithic fragments. Otowi Member ignimbrite is not exposed in the quadrangle north of Rendija Canyon, probably due to a lack of deposition; however,

about 1 to 3 m of the basal Plinian tephra, the Guaje Pumice Bed, is preserved to the north. In canyons north of Rendija Canyon, such as Cabra Canyon and Guaje Canyon, Cerro Toledo deposits typically rest directly upon Guaje Pumice with no intervening Otowi Member tuff. South of Rendija and Barrancas canyons, the Otowi Member thickens significantly in Bayo and Pueblo canyons in the southeast corner of the quadrangle.

A small hill that lies just to the north of Rendija Canyon near the eastern edge of the quadrangle preserves key stratigraphic relationships. Beneath the hill, Puye Formation conglomerates underlie poorly exposed Cerro Toledo and Guaje tephras, with a break in slope defining the contact between the units. On the north side of the hill there is a small vestige of upper Bandelier Tuff. An unconsolidated gravel deposit that probably temporally correlates to the Cerro del Medio pumice-bearing Qalo deposits in the western part of Rendija Canyon sits on the Tshirege Member; however, this old alluvium deposit contains a different mix of clasts compared to the Qalo deposits in North Community (Table 2). These deposits are generally more coarse-grained and contain little pumice. The clasts are dominantly Tschicoma Formation lavas, but flow-banded rhyolite, rhyolite, obsidian, and black, glassy Tshirege Member tuff are common, as well. The rhyolitic component is most likely from the Toledo embayment near the headwaters of Guaje Canyon. The distribution of old alluvium in the vicinity of Rendija and Guaje canyons suggests that paleo-Guaje Canyon flowed north and east of Guaje Mountain, forming a broad alluvial fan prior to establishing its current narrow and circuitous course.

### **Guaje Canyon**

Guaje Canyon forms a deep (locally >300 m) canyon that provides an important east-west stratigraphic profile in the quadrangle (Figure 2). The headwaters are carved into thick, possibly near-source facies of Tschicoma Formation dacite lavas (Ttrc and Ttcm). An eastward-thickening wedge of Puye Formation (Tp) fanglomerates overlies the lavas, forming most of the lower canyon walls down canyon. In turn, younger Guaje Pumice Bed, Cerro Toledo deposits (Qct), and upper Bandelier Tuff (Qbt) overlie the fanglomerates. The stratigraphic sequence is capped by isolated exposures of mesa-top alluvium (Qalo) that was deposited prior to canyon incision.





*View east of the water gap cut through the rhyodacite of Rendija Canyon by Guaje Creek.*

Caballo Mountain rises 600 m above the Guaje Canyon floor near the western margin of the quadrangle. The ~5 Ma rhyodacite of Rendija Canyon may have erupted from a source west of the quadrangle. The  $3.03 \pm 0.15$  Ma dacite of Caballo Mountain (Broxton et al., 2007) appears to have originated from a vent at Caballo Mountain. The rhyodacite of Rendija Canyon exceeds 300 m in thickness on the southern wall of Guaje Canyon and thins gradually to the south along Sierra de Los Valles. Flow breaks in the rhyodacite form topographic benches on the south side of Guaje Canyon, and some of those benches are covered with Tshirege Member or by terrace gravels. Thick exposures of rhyodacite also occur along the east flanks of Caballo Mountain in the Vallecitos and Vallecito de los Caballos drainages. These lavas are capped by the younger dacite of Caballo Mountain, which filled steep valleys cut into the older Rendija Canyon lavas and flowed eastward. Locally, the dacite of Caballo Mountain appears to overlie Puye Formation sediments. One of the main Caballo Mountain lava flows extended to the NE toward the Pine Springs area (see discussion on Pine Springs geology). A branch from this flow lobe is exposed in the Vallecitos valley. Much of the Tschicoma Formation is undifferentiated north of Guaje Canyon, due to region's rugged topography and unavailable access to Santa Clara Pueblo land.

An interesting, isolated outcrop of tephra overlain by ignimbrite occurs in Guaje Canyon at UTM coordinates 376950E 3977320N (NAD 27). This tephra and ignimbrite, mapped as Tti, is of unclear origin and stratigraphic position, as no overlying rocks, except for colluvium, occur at the outcrop. The deposit may be of Tschicoma Formation age, erupted between lava flows, or it may be much younger, deposited during a small-

volume, intracaldera eruption that postdates the Valles caldera ( $< 1.22$  Ma). A second ignimbrite deposit that is about 6 m thick is exposed on the south side of Guaje Canyon between 380520E 39977200N and 380750E 3977180N (NAD 27). This tuff appears to be in the Puye Formation.



Ignimbrites in Puye Formation in Guaje Canyon at 380750E 3977180N (NAD 27).

The Rendija Canyon fault crosses Guaje Canyon near the confluence of three large drainages: Guaje Canyon, Vallecitos Canyon, and Agua Piedra Canyon. Upper Bandelier Tuff exposed on mesa tops north and south of the confluence show at least 12 m of down-to-the-west offset. Significantly more offset of older units along the fault is implied by the juxtaposition of Puye Formation sediments and Caballo Mountain dacite in the north canyon wall. However, a perched Quaternary terrace deposit overlying Puye deposits near the intersection of the three canyons shows no apparent offset by the fault, suggesting very little movement of this segment of the fault in the late Quaternary. A fault sub-parallel to the Rendija Canyon fault occurs approximately 0.6 km to the east. This fault, which also displays down-to-the-west displacement, extends south to Cabra

Canyon, just north of Rendija Canyon. Between the two faults, a ridge capped by upper Bandelier Tuff extends into Guaje Canyon. This ~ E-W-trending ridge coincides with the axis of a small paleocanyon for the upper Bandelier Tuff. On the mesa due north from this ridge, the base of the tuff is > 120 m higher in elevation, whereas the base of the tuff is ~60 m higher on mesas to the south. No E-W faults bound the ridge to provide an alternative explanation for this topographic variance.



In this same general vicinity, a colluvial wedge composed of eroded Bandelier Tuff and a gravel deposit are preserved on downthrown side of the Rendija Canyon fault on top of the low-elevation E-W ridge discussed above. This deposit lines up with a southeast-trending string of alluvial deposits (Qalo2) composed of cobbles to boulders of Tschicoma Formation lava and rounded Tshirege Member tuff that are cutting into Cerro Toledo deposits subparallel to the modern trend of upper Cabra Canyon. A shallow, southeast-trending, early Pajarito Plateau drainage developed in upper Cabra Canyon, but it was cut off by a now deeply incised, southwest-trending unnamed tributary to Guaje Canyon.

East of the Rendija Canyon fault, a pronounced bench occurs at the top of the Puye Formation, with overlying Guaje Pumice Bed, Cerro Toledo, and upper Bandelier Tuff deposits recessively backwasted to varying degrees. This remarkably planar bench continues eastward to the east edge of the quadrangle. An outcrop of red, altered, finely

porphyritic dacite is exposed on the north side of Guaje Canyon between the Rendija Canyon and Guaje Mountain fault zones. The rock yielded a  $^{40}\text{Ar}/^{39}\text{Ar}$  age of  $9.58 \pm 0.13$  Ma.

At the intersection of Guaje Canyon with the Guaje Mountain fault, Guaje Canyon makes two short right angle bends, passes through a narrow constriction between two peaks of Rendija Canyon rhyodacite (Guaje Mountain to the south), then continues eastward to the edge of the quadrangle. This double bend in the canyon was likely established shortly after the deposition of the Bandelier Tuff as incipient east-west canyons forming. Possibly, stream capture was involved, with two subparallel E-W drainages forming on either side of the northern Tschicoma lava peak. Once the southern E-W drainage eroded through the notch between the two lava peaks, it may have migrated the short distance northward to capture the northern E-W drainage.

Remnants of an early Pajarito Plateau alluvial fan is preserved both north and south of Guaje Canyon. The fan apparently went around the north side of the northern Tschicoma Formation peak east of the Guaje Mountain fault. The clasts in this old alluvium are similar to those described earlier (Table 2) and point toward a source in the headwaters of Guaje Canyon west of the quadrangle boundary.

Substantial vertical offset along the Guaje Mountain fault has occurred since the emplacement of the upper Bandelier Tuff in the vicinity of Guaje Canyon. To the north, approximately 14 m of down-to-the-west offset has occurred. To the south, upper Bandelier Tuff is juxtaposed against Tschicoma Rendija Canyon lavas along the fault, so offset is difficult to determine. Much greater offset is implied by offset of the Tschicoma Formation lavas along the fault at Guaje Mountain, with perhaps  $> 120$  m of down-to-the-west displacement. Recent fault kinematic studies by Gardner et al (2003) based on analysis of rocks exposed in three trenches across and in the hanging wall of the fault in Chupadera Canyon, just north of Guaje Canyon, indicate that a left-lateral strike-slip event with  $< 0.5$  m of vertical displacement occurred about 39 ka. Faulting disrupts 10 ka alluvium in one of the trenches.

### **Pine Spring**

Pine Spring is located along the northern extension of the Guaje Mountain fault where several tributary canyons converge to mark the beginning of Garcia Canyon

(Figure 3). Native American and other human settlers in the region have used the spring for hundreds of years and the Forest Service at one time had a field station there (Martin, 1998). The area is of particular geologic interest since most of the major rock units in the quadrangle outcrop within a small 1 km<sup>2</sup> area around the springs.

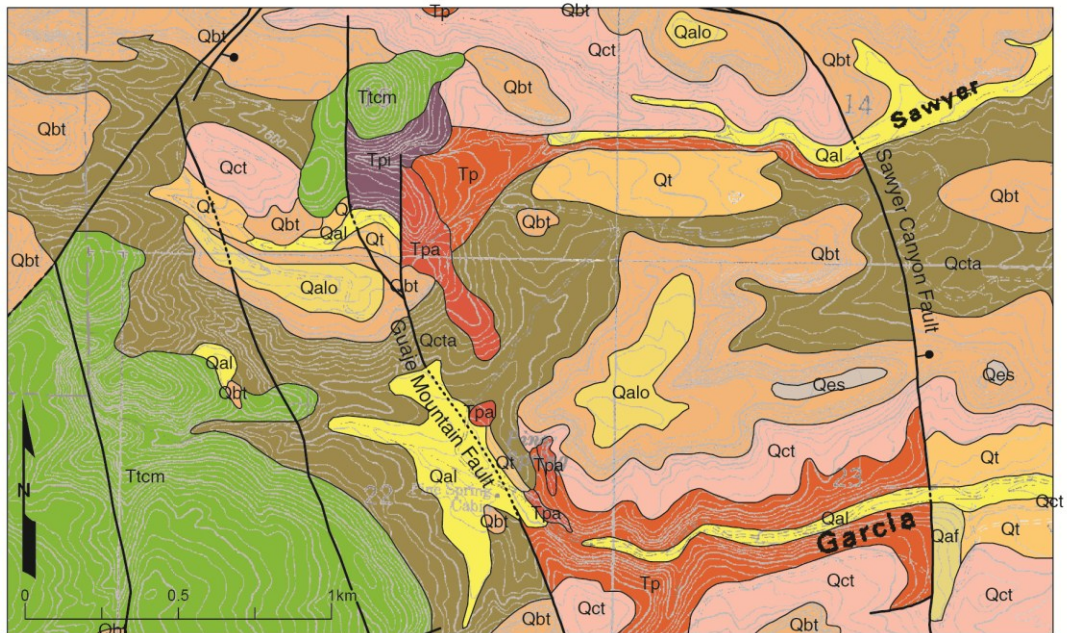


Figure 3. Simplified geologic map showing the distribution of major rock units in the Pine Spring area.

The oldest rocks in the quadrangle, mid-Miocene age andesitic lavas (Tpa), crop out on the east side of the Guaje Mountain fault near the spring and on the footwall of the Pararito fault zone north of the spring. These lavas, along with similar outcrops in Los Alamos Canyon and Guaje Canyon, likely represent rift-related intermediate composition volcanic activity in the area in the area between 9-13 Ma (WoldeGabriel et al., 2001). A large distal flow lobe of Tschicoma Caballo Mountain lava (Tcm), which forms a broad 50 m-high escarpment immediately west of the springs, represents the next youngest rocks in the area. Continuous outcrops of this flow to the west suggest an origin along the north slope of Caballo Mountain. An ignimbrite with Caballo Mountain dacite lithics is exposed along the north side of the Caballo Mountain dacite knob; the chemistry of the pumice in that deposit is in Table 1. Comparably-aged Puye Formation fanglomerates comprise the north wall of Garcia Canyon just east of the springs, overlapping the

andesitic lavas. Most of the valley floor in the vicinity of the springs is interpreted to be Cerro Toledo Formation (Qct / Qcta), including reworked tephras and Puye conglomerates. However, the reworked nature of these sediments, in combination with Puye-like recent terrace deposits, makes stratigraphic placement of the valley-fill difficult to interpret with certainty. Above the valley floor, primary Cerro Toledo tephra deposits are exposed, cropping out below the upper Bandelier Tuff in cliff exposures south, east, and north of the springs. The overlying upper Bandelier Tuff is typically underlain by ~1 m of Tsankawi pumice. Finally, on a Bandelier Tuff mesa just NE of the springs, mesa-capping Quaternary gravels complete the local stratigraphic section.

Cerro Toledo deposits west of Pine Springs include thick sequences of Puye-like conglomerates, capped by tephra deposits that shortly preceded the eruption of the upper Bandelier Tuff. These deposits, which contain distinctive clasts of aphyric obsidian, thicken westward, filling a paleovalley between dacite of Caballo Mountain highlands. Sedimentation continued in this area after the emplacement of the upper Bandelier Tuff, evidenced by a thick gravel cap on the tuff.

The Guaje Mountain fault bends to the northwest in the Pine Springs area and can be traced into the south side of a large topographic knob of Tschicoma Caballo lava. The andesites and the Puye conglomerates are offset by the fault (down-to-the-west), although no estimate for displacement of these units could be determined. Displacement along the fault appears to taper to the north, as upper Bandelier Tuff south of the springs is offset by at least 30 m while tuff deposits north of the springs are offset by < 3 m.

### **Sawyer Canyon fault**

The Sawyer Canyon fault is the easternmost fault in the Guaje Mountain quadrangle. This down-to-the-east fault trends southeast to south and marks the east side of a horst; the Guaje Mountain fault defines the west side of the horst. Near the eastern edge of the quad, one splay of the Sawyer Canyon fault bends sharply to the east, while several small-displacement splays continue to the south, intersecting both Guaje and Rendija canyons. Cerro Toledo tephras are quite thick (24 to 30 m) and sandstone beds are rare in this deposit on the downthrown side of the Sawyer Canyon fault. Just east of the fault south of Chupaderos Canyon, Cerro Toledo deposits not capped by Tshirege Member are covered with Puye-like alluvial fan gravel. Rounded Tschicoma clasts are

eroding out of the Puye Formation exposed on the footwall of the Sawyer Canyon fault and are then deposited as alluvial fan gravel on the Cerro Toledo deposits. Similar alluvial fan and terrace gravels are present in Garcia Canyon.



View of the monoclinical offset of the Tshirege Member of the Bandelier Tuff by the Sawyer Canyon fault, looking toward the northwest. White line marks the approximate trace of the fault. The area in the foreground is underlain by Cerro Toledo tephra capped by Puye-like alluvial fan gravels.

## References

- Bailey, R.A., Smith, R.L. Ross, C.S., 1969, Stratigraphic nomenclature of volcanic rocks in the Jemez Mountains, New Mexico: U.S. Geological Survey Bulletin, 1274, p. 1-19.
- Broxton, D.E., and Reneau, S.L., 1995, Stratigraphic nomenclature of the Bandelier Tuff for the Environmental Restoration Project at Los Alamos National Laboratory: Los Alamos National Laboratory, Report LA-13010-MS, 21 p.
- Broxton, D.E. and Reneau, S.L., 1996, Buried early Pleistocene landscapes beneath the Pajarito Plateau, Northern New Mexico: New Mexico Geological Society, 47<sup>th</sup> Field Conference Guidebook, p. 325-334.
- Broxton, D.E., and Vaniman, D.T., 2005, Geologic framework of a groundwater system on the margin of a rift basin, Pajarito Plateau, north-central New Mexico: Vadose Zone Journal, v. 4, p. 522-550.
- Broxton, D., WoldeGabriel, G., Peters, L., Budahn, J., and Kluk, E., 2007, Pliocene volcanic rocks of the Tschicoma Formation, east-central Jemez volcanic field: Chemistry, petrography, and age constraints: New Mexico Geological Society, 58<sup>th</sup> Field Conference, Guidebook, p. 284-295.
- Gardner, J.N., and Goff, F., 1996, Geology of the northern Valles caldera and Toledo Embayment, New Mexico: New Mexico Geological Society, 47<sup>th</sup> Field Conference, Guidebook, p. 225-230.
- Gardner, J.N., Goff, E, Garcia, S., and Hagan, R.C., 1986, Stratigraphic relations and lithologic variations in the Jemez volcanic field, New Mexico: Journal of Geophysical Research, v. 91, p. 1763-1778.
- Gardner, J.N., Goff, F., Reneau, S.L., Sandoval, M.M., Drakos, P.G., Katzman, D., and Goff, C.J., 2006, Preliminary geologic map of the Valle Toledo quadrangle, Los Alamos and Sandoval Counties, New Mexico: New Mexico Bureau of Geology and Mineral Resources, Open-file Geologic Map OF-GM 133, scale 1:24,000.
- Gardner, J. N., Lavine, A., WoldeGabriel, G., Vaniman, D., 1998, High-precision geologic mapping to evaluate the potential for seismic surface rupture at TA-55, Los Alamos National Laboratory; Los Alamos National Laboratory Report, LA-13456-MS, 13 p.

- Gardner, J. N., Lavine, A., WoldeGabriel, G., Krier, D. J., Vaniman, D., Caporuscio, F., Lewis, C., Reneau, P., Kluk, E., and Snow, M. J., 1999, Structural geology of the northwestern portion of Los Alamos National Laboratory, Rio Grande rift, New Mexico: Implications for seismic surface rupture potential from TA-3 to TA-55: Los Alamos National Laboratory Report, LA-13589-MS, 112 p.
- Gardner, J.N., Reneau, S.L., Lavine, A., Lewis, C.J., Katzman, D., McDonald, E.V., Lepper, K., Kelson, K.I., and Wilson, C., 2003, Paleoseismic trenching in the Guaje Mountain fault zone, Pajarito fault system, Rio Grande rift, New Mexico: Los Alamos National Laboratory Report LA-14087-MS, 68 pp.
- Goff, F., Gardner, J.N., and Reneau, S.L., 2001, Geology of the Frijoles 7.5-minute quadrangle, Los Alamos, Santa Fe and Sandoval Counties, New Mexico: New Mexico Bureau of Geology and Mineral Resources, Open-file Geologic Map OF-GM 42, scale 1:24,000.
- Griggs, R.L., 1964, Geology and ground-water resources of the Los Alamos area, New Mexico: United States Geological Survey, Water-Supply Paper 1753, 107 p.
- Heiken, G., Goff, F., Stix, J., Tamanyu, S., Shafiqullah, M., Garcia, S. and Hagan, R., 1986, Intracaldera volcanic activity, Toledo caldera and embayment, Jemez Mountains, New Mexico: *Journal of Geophysical Research*, v. 91 (B2), p. 1799-1815.
- Kelson, K., Hemphill-Haley, M., Olig, S., Simpson, G., Gardner, J., Reneau, S., Kolbe, T., Forman, S., and Wong, I., 1996, Late Pleistocene and possibly Holocene displacement along the Rendija Canyon fault, Los Alamos County, New Mexico: *New Mexico Geological Society Guidebook 47*, p. 153-160.
- Izett, G.A. and Obradovich, J.D., 1994,  $^{40}\text{Ar}/^{39}\text{Ar}$  age constraints for the Jaramillo normal subchron and the Matayama-Brunhes geomagnetic boundary: *Journal of Geophysical Research*, v. 99(B2), p. 2925-2934.
- Izett, G., Obradovich, J., Naeser, C., and Cebula, G., 1981, Potassium-argon and fission-track zircon ages of Cerro Toledo rhyolite tephra units in the Jemez Mountains, New Mexico: U.S. Geological Survey, Professional Paper 1199-D, p. 37-43.
- Le Bas, M.J., Le Maitre, R.W., Streckeisen, A., and Zanettin, B., 1986, A chemical classification of volcanic rocks based on the total alkali-silica diagram: *Journal of Petrology*, v. 27, p. 745-750.

- Lavine, A., Lewis, C.J., Katcher, D.K., Gardner, J.N., and Wilson, J., 2003, Geology of the north-central to northeastern portion of Los Alamos National Laboratory, New Mexico: Los Alamos National Laboratory Report LA-14043-MS, 44 p.
- Lewis, C.J., Lavine, A., Reneau, S.L., Gardner, J.N., Channell, R., and Criswell, C.W., 2002, Geology of the western part of Los Alamos National Laboratory (TA-3 to TA-16), Rio Grande rift, New Mexico: Los Alamos National Laboratory Report LA-13960-MS, 98 p.
- Martin, C., 1998, Los Alamos place names: Los Alamos Historical Society, Los Alamos, New Mexico, 126 pp.
- McCalpin, J.P., 1998, Late Quaternary faulting on the Pajarito fault, west of Los Alamos National Laboratory, north-central New Mexico: Results from the seven-trench transect excavated in summer of 1997: unpublished consulting report prepared for Los Alamos National laboratory by GEO-HAZ Consulting Inc., Estes Park, Colorado.
- Olig, S., Kelson, K., Gardner, J., Reneau, S., and Hemphill-Haley, M., 1996, The earthquake potential of the Pajarito fault system, New Mexico: New Mexico Geological Society Guidebook 47, pp. 143-151.
- Phillips, E. H., 2004, Collapse and resurgence of the Valles caldera, Jemez Mountains, New Mexico:  $^{40}\text{Ar}/^{39}\text{Ar}$  age constraints on the timing and duration of resurgence and ages of megabreccia blocks [M.S. thesis]: Socorro, New Mexico Institute of Mining and Technology, 200 p.
- Phillips, W.M., McDonald, E.V., Reneau, S.L., and Poths, J., 1998, Dating soils and alluvium with cosmogenic  $^{21}\text{Ne}$  depth profiles: Case studies from the Pajarito Plateau, New Mexico, USA: Earth and Planetary Science Letters, v. 160, p. 209-223.
- Reneau, S. L., 2000, Stream incision and terrace development in Frijoles Canyon, Bandelier National Monument, New Mexico, and the influence of lithology and climate: Geomorphology, v. 32, p. 171-193.
- Reneau, S.L., and Dethier, D.P., 1996, Pliocene and Quaternary history of the Rio Grand, White Rock Canyon and vicinity, New Mexico: New Mexico Geological Society, 47<sup>th</sup> Field Conference, Guidebook, p. 317-324.

- Reneau, S. L., and Dethier, D. P., 1996b, Late Pleistocene landslide-dammed lakes along the Rio Grande, White Rock Canyon, New Mexico: Geological Society of America Bulletin, v. 108, p. 1492-1507.
- Reneau, S. L., and McDonald, E. V., 1996, Landscape history and processes on the Pajarito Plateau, northern New Mexico: Rocky Mountain Cell, Friends of the Pleistocene, Field Trip Guidebook, Los Alamos National Laboratory report LA-UR-96-3035, 195 p.
- Reneau, S.L., Gardner, J.N. and Forman, S.L., 1996, New evidence for the age of the youngest eruptions in the Valles caldera, New Mexico: Geology, v. 24, p. 7-10.
- Reneau, S.L., Kolbe, T.R., Simpson, D.T., Carney, J.S., Gardner, J.N., Olig, S.S., and Vaniman, D.T., 1995, Surficial materials and structure at Pajarito Mesa, *in* Reneau, S.L., and Raymond, R., eds., Geological site characterization for the proposed Mixed Waste Disposal Facility, Los Alamos National Laboratory: Los Alamos National Laboratory Report LA-13089-MS, p. 31-69.
- Reneau, S.L., Gardner, J.N., Lavine, A., McDonald, E.V., Lewis, C., Katzman, D., WoldeGabriel, G., Krier, D., Berfeld, D., and Heikoop, J., 2002, Paleoseismic investigation of trench EOC-2, Pajarito fault zone, Los Alamos National Laboratory, New Mexico: Los Alamos National Laboratory Report LA-13939-MS, 65 p.
- Rogers, M.A., 1995, Geologic map of Los Alamos National Laboratory Reservation: State of New Mexico Environment Department, scale 1:400, 21 p.
- Samuels, K.E., Broxton, D.E., Vaniman, D.T., WoldeGabriel, G., Wolff, J.A., Hickmott, D.D., Kluk, E.C, Fittipaldo, M.M., 2007, Distribution of dacite lavas beneath the Pajarito Plateau, Jemez Mountains, NM: New Mexico Geological Society, 58<sup>th</sup> Field Conference, Guidebook, p. 296-307.
- Smith, R.L., and Bailey, R.A., 1966, The Bandelier Tuff: a study of ash-flow eruption cycles from zoned magma chambers: Bulletin Volcanologique, v. 29, p. 83-104.
- Smith, R.L., Bailey, R.A., and Ross, C.S., 1970, Geologic map of the Jemez Mountains, New Mexico: U. S. Geological Survey, Miscellaneous Geologic Investigations, I-571, scale 1:125,000.
- Spell, T.L., 1987, Geochemistry of the Valle Grande Member ring fracture rhyolites, Valles caldera, New Mexico [M.S. thesis]: Socorro, New Mexico Institute of Mining and Technology, 212 p.

- Spell, T.L., and Harrison, T.M., 1993,  $^{40}\text{Ar}/^{39}\text{Ar}$  geochronology of post-Valles caldera rhyolites, Jemez volcanic field, New Mexico. *J. Geophysical Research*, v. 98, p. 8031-8051.
- Spell, T.L., McDougall, I. and Doulgeris, A.P., 1996, The Cerro Toledo Rhyolite, Jemez Volcanic Field, New Mexico:  $^{40}\text{Ar}/^{39}\text{Ar}$  geochronology of eruptions between two caldera-forming events. *Bulletin Geological Society America*, 108, 1549-1566.
- Stix, J., 1989, Physical and chemical fractionation processes in subaerial and subaqueous pyroclastic rocks [Ph.D. dissertation]: University of Toronto, 420 p.
- Stix, J., Goff, F., Gorton, M., Heiken, G., and Garcia, S., 1988, Restoration of compositional gradients in the Bandelier silicic magma chamber between two caldera-forming eruptions. *J. Geophys. Res.*, v. 93, p. 6129-6147.
- Turbeville, B.N., Waresback, D.B., Self, S., 1989, Lava-Dome growth and explosive volcanism in the Jemez Mountains, New Mexico: Evidence from the Plio-Pleistocene Puye alluvial fan: *Journal of Volcanology and Geothermal Research*, v. 36, p. 267-291.
- Waresback, D., 1986, The Puye Formation, New Mexico: Analysis of a continental rift-filling volcanoclastic alluvial fan sequence. M.S. thesis, Univ. Texas, Arlington, 225 pp.
- Wells, D. and Coppersmith, K.J., 1994, New earthquake magnitude and fault rupture parameters, correlations among earthquake magnitude, rupture length, and fault displacement: *Bulletin of the Seismological Society of America*, v. 84, p. 974-1002.
- Wong, I., Kelson, K., Olig, S., Bott, J., Green, R., Kolbe, T., Hemphill-Haley, M., Gardner, J., Reneau, S., and Silva, W., 1996, Earthquake potential and ground shaking hazard at the Los Alamos National Laboratory, New Mexico: *New Mexico Geological Society Guidebook 47*, pp. 135-142.
- WoldeGabriel, G., Warren, R.G., Broxton, D., Vaniman, D.T., Heizler, M., Kluk, E., and Peters, L., 2001, Episodic volcanism, petrology, and lithostratigraphy of the Pajarito Plateau and adjacent areas of the Española basin and the Jemez Mountains, in Crumpler L.S., and Lucas, S.G., Eds., *Volcanology in New Mexico: New Mexico Museum of Natural History and Science Bulletin*, 18, p. 97-129.

WoldeGabriel, G., Warren, R.G., Cole, G., Goff, F., Broxton, D., Vaniman, D., Peters, L., Naranjo, A., and Kluk, E., 2006, Volcanism, tectonics, and chronostratigraphy in the Pajarito Plateau of the Española Basin, Rio Grande rift, north central New Mexico, USA, Los Alamos National Laboratory, LA-UR-06-6089, 122 p.

## Appendix I

### Unit Descriptions – Guaje Mountain 7.5-Minute Quadrangle

**Qal – Alluvium.** Silt, sand and gravel deposited in modern drainages; may include terrace deposits. Streams draining the Sierra de Los Valles are particularly laden with sand and gravel of the rhyodacite or dacite derived from the Tschicoma Formation; stream deposits within the Pajarito Plateau contain abundant clasts and phenocryst grains of the Bandelier Tuff. Holocene to Pleistocene in age (Phillips et al., 1998; Reneau, 2000) with a maximum thickness of ~ 5 meters.

**Qes – Eolian and sheet wash deposits.** Tan to brown silt-to clay- rich soil that develops primarily on Cerro Toledo interval on the east side of the map area. Soil material is transported in by the wind, but is reworked by slope wash. Holocene to Pleistocene in age with an average thickness of ~ 1 meter.

**Qc – Colluvium.** Talus debris that typically form wedge-shaped deposits adjacent to cliffs (in particular the Tshirege Member of the Bandelier Tuff, **Qcbt**). Debris is unsorted to poorly-sorted, often obscuring faults and/or contacts between rock units. Although abundant, these deposits were mapped in only a few locations, particularly on north facing slopes. Holocene to Pleistocene in age with a maximum thickness of ~ 15 meters.

**Qvec – El Cajete Pyroclastic Beds, East Fork Member, Valles Rhyolite.** White to beige pyroclastic fall deposits containing pumice, ash, crystals, and lithic fragments. The pumice contains < 10% phenocrysts of quartz sanidine, and biotite. The deposits in this area are not primary, but are reworked. 50 to 60 ka (Reneau et al., 1996). < 1 m thick.

**Qt- Terrace gravel.** Fluvial pebble to boulder-sized gravel composed primarily of Tschicoma Formation lava or Bandelier Tuff, deposited along the edges of modern drainages at levels as much as 30 m above the present canyon floor. Terraces are particularly well developed in Rendija Canyon (Reneau and McDonald, 1996; Reneau et al., 1996). Terraces are also well preserved in eastern Pueblo Canyon, Guaje Canyon, and Sawyer Canyon. El Cajete pumice sits on a low terrace on the south side of Pueblo Canyon near the eastern edge of the map. Holocene to Pleistocene in age (Reneau, 2000) with a maximum thickness of ~ 30 meters. In Pueblo Canyon **Qt1** is the higher terrace level; **Qt2** is lower. El Cajete pumice overlies Qt2 at the eastern edge of the quadrangle.

**Qaf - Alluvial fan deposits.** Tan silt and gravel overlying Cerro Toledo deposits or Bandelier Tuff east of the Sawyer Canyon and Pajarito fault zones in the eastern part of the map area. The gravel is derived from Puye Formation eroding from the footwall of the faults. Pleistocene in age and ~1- 3 meter thick.

**Qls – Landslides.** Two types: slump or block slides that remain nearly intact after detaching from a steep slope or cliff, or unsorted, chaotic debris emplaced during a chaotic detachment event from a steep slope or cliff. The latter deposits are typically fan-shaped on the valley floor. Holocene to Pleistocene in age of highly variable thicknesses.

**Qcta – Cerro Toledo deposits (see below) with younger alluvium and/or colluvium, undivided.** These deposits typically occur in valleys where the upper portions of the underlying Cerro Toledo tephras have been reworked and are mixed with younger alluvial and colluvial material. Younger material typically includes reworked vitric pumices of Bandelier Tuff (Tsankawi or Tshirege Member) or clasts of devitrified Bandelier Tuff. Alluvial material may also include younger terrace deposits, with rounded cobbles and boulders of Tschicoma lavas.

**Qalo<sub>2</sub> – Old alluvium.** Clasts of rounded Tshcioma Formation dacite to rhyodacite and rounded Bandelier Tuff preserved in a southeast-trending paleochannel cut into Cerro Toledo deposits in upper Cabre Canyon.

**Qalo – Older alluvium.** In the town site of Los Alamos, this unit is largely composed of alternating gravel and sandstone layers of fluvial origin interbedded with beds of tephra. Some gravel lenses are dominated by pumice, but most lenses contain subequal amounts of pumice and Tshcioma Formation lava, and rare flow-banded rhyolite and obsidian granule- to pebble-sized gravel. The tephra beds are <1 m thick; the pumice is likely derived from the Cerro del Medio dome to the west of Los Alamos erupted at ~ 1.1 Ma (Spell and Harrison, 1993). The older alluvium is well exposed in a road cut just southwest of the Larry R. Walkup Aquatic Center on Canyon Road in Los Alamos. Northeast of Los Alamos, the unit is dominantly gravel, including clasts of Bandelier Tuff; pumice is absent in these deposits. The older alluvium generally sits on Bandelier Tuff. North of Los Alamos, Qalo contains abundant clasts of streaky, flow-banded rhyolite lava, black, grassy tuff, and some obsidian. Qalo was deposited as fans shortly after the eruption of the Bandelier Tuff prior to the development of the modern drainage system (Reneau). Pleistocene in age with a maximum thickness of ~ 30 meters.

**Qbt – Upper Bandelier Tuff, Tshirege Member.** Beige to orange to gray, poorly-welded to densely-welded ignimbrite containing abundant phenocrysts of sanidine and quartz and trace amounts of clinopyroxene and hypersthene (Smith and Bailey, 1966). Sanidine commonly displays blue iridescence. Accidental lithic fragments typically < 5% except in discreet lenses and lag horizons. Qbt is a compound flow unit with multiple flow units as described by Broxton and Reneau (1995) and Gardner et al. (1999, 2001), and is well exposed in canyons throughout the Pajarito Plateau. Surge deposits, typically < 1 meter thick, are common at the base of the unit and overlie a stratified pumice tephra (Tsankawi Pumice Bed) that is typically ~ 1 meter thick. The ignimbrite was erupted from the Valles caldera at 1.25±0.01 Ma (Phillips, 2004) and filled valleys along the paleotopographically complex eastern flank of Sierra de Los Valles. The degree of welding decreases toward east and some of the upper cooling units pinch out toward the east. Maximum observed thickness is ~ 180 meters.

**Qct – Cerro Toledo deposits.** Tephra, reworked tephra and epiclastic alluvium deposited between eruptions of the Tshirege and Otowi members of the Bandelier Tuff (Broxton and Reneau, 1995). Alluvial deposits include sand, silt, and conglomerates with rounded clasts of Tschicoma lavas. Aphyric obsidian common. Fanglomerate alluvial deposits in Los Alamos Canyon record a major fluvial system during this interval. Tephra originated from rhyolite dome complex eruptions in the Toledo caldera and the Toledo embayment (Smith et al., 1970; Heiken et al., 1986). Tephra deposits typically contain pumices with rare phenocrysts of quartz, sanidine and biotite. In the northern portion of the map area crystal-rich tephra occur near the top of the interval, with abundant phenocrysts of quartz and sanidine. Radiometric ages of pumices and source domes range from 1.21 to 1.64 Ma (Izett et al., 1981; Stix et al., 1988; Spell et al., 1996). Maximum exposed thickness is ~ 100 meters.

**Qbo – Lower Bandelier Tuff, Otowi Member.** White to beige poorly-welded ignimbrite with abundant phenocrysts of quartz and sanidine (Bailey et al., 1969). Abundant accidental lithic fragments of dark grey to red mafic rocks give outcrops a peppered appearance. Qbo is primarily a slope-forming unit and was erupted from the Toledo caldera at  $1.61 \pm 0.01$  to  $1.62 \pm 0.04$  Ma (Izett and Obradovich, 1994; Spell et al., 1996). Otowi Member ignimbrite was deposited primarily in the southeastern portion of the quadrangle and was not deposited north of Rendija Canyon. The Guaje Pumice Bed, a stratified pumice fall and surge deposit that preceded Otowi ignimbrite deposition, is exposed in isolated outcrops in Cabra Canyon (**Qbog**) and beneath the Otowi Member in Pueblo Canyon. The Guaje Pumice Bed, which is 2 - 3 m thick also crops out the contact between the Puye Formation and Cerro Toledo deposits in Guaje Canyon. Maximum exposed thickness is ~ 50 m.

**Tp/Tpi – Puye Formation.** Light to dark gray fanglomerates derived from Tschicoma lavas (Griggs, 1964; Gardner et al., 1986; Waresback, 1986; Turbeville et al., 1989). Silt and sand layers interbedded with cobble to boulder-sized conglomerates deposited as debris flows, lahars, and alluvial fans. Clasts are typically rounded to sub-rounded and include a wide variety of dacitic and rhyodacitic lavas. Rhyodacite of Rendija Canyon and dacite

of Caballo Mountain clasts are common. Lower Puye Formation deposits that overlie Santa Fe Group sediments east of the study area include clasts of rhyodacite of Rendija Canyon, suggesting a major eastward progradation of Puye Formation following the eruption of the Rendija Canyon rhyodacite at ~ 5.0 Ma. Reneau and Dethier (1996) note that deposition of the Puye Formation was probably controlled by blockage of the Rio Grande by volcanism in the Cerros del Rio volcanic field located to the southeast of the quadrangle. Age range of exposed Puye Formation is ~ 2.4 to 5.3 Ma (WoldeGabriel et al., 2001). Maximum thickness is ~ 100 meters.

Thin beds of tephra and/or ignimbrites (**Tpi**) are interbedded with these sediments. In the middle reaches of Guaje Canyon, on the south side of the canyon, <0.5 m layers of tephra and ignimbrite are interbedded; the entire deposit is 6 to 10 m thick. The contact relations in the middle portion of Guaje Canyon are obscure, but this deposit appears to lie between Rendija Canyon rhyodacite and Puye Formation. The tan ignimbrite contains abundant gray pumice fragments, quartz, sanidine, obsidian, and lithic fragments. A second set of exposures occurs on the south side of Guaje Canyon along the old road into the canyon. One tephra is exposed near the canyon bottom and one is near the top of the Puye Formation. The upper tephra gives a  $^{40}\text{Ar}/^{39}\text{Ar}$  age of  $4.01 \pm 0.22$  Ma. The tephra is clast-supported pumice fall < 1 m thick. Clasts range in size from 0.5-1.0 cm. Clots of large (1-3 mm), fresh, euhedral amphibole crystals are present throughout the sample. Some clots include small, uncommon felsic minerals that are impossible to identify using a binocular microscope. Other clots have rare occurrences of biotite, but, for the most part, these clots are monomineralic. Lithics include light gray clasts of glassy and stony lava. Clay is pervasive as an alteration product, but a gritty texture suggests that primary glass may still be present. Maximum thickness is ~ 6 meters.

### **Tschicoma Formation (Pliocene).**

**Ttnd – “Northern dacites”, Tschicoma Formation (shown only on cross-section B-B’).** Crystal poor dacite with 2-5% phenocrysts of plagioclase, clinopyroxene and orthopyroxene encountered in well H-19.  $^{40}\text{Ar}/^{39}\text{Ar}$  ages of  $2.36 \pm 0.54$  and  $2.49 \pm 0.23$  Ma have been determined from similar lavas in a drillhole to the south of the quadrangle (Samuels et al., 2007; Broxton et al., 2007).

**Ttcm – Dacite of Caballo Mountain, Tshicoma Formation.** Lavender to dark gray flow-banded dacitic lavas and associated block and ash flows erupted from the vicinity of Caballo Mountain. Streaky, flow-banded lavender to red facies common. Lavas contain 10–20% phenocrysts of plagioclase and hornblende with subordinate pyroxene, biotite and quartz. At least three separate flows occur, the youngest containing more abundant hornblende. These flows extended in two main directions: one extending SSE of Caballo Mountain, capping the north canyon wall of Guaje Canyon, and one that flowed to the ENE of Caballo Mountain, extending to just west of Pine Springs. Sample from top of Caballo Mountain has age date of  $3.03 \pm 0.15$  Ma (Broxton et al., 2007))

**Ttca – Small volume tephra, ignimbrites, block and ash flows, and associated colluvial deposits.** Outcrops are limited to exposures ~ 0.5 km NNW of Pine Springs. Glassy lava fragments in the block and ash flows appear dacitic, with phenocrysts of plagioclase, amphibole, pyroxene and biotite. Stratified tephra and ignimbrite facies dip ~15° in an easterly direction. These deposits appear to be overlain by Caballo Lavas and are therefore likely to be > 3.0 Ma. Maximum thickness is ~ 30 meters.

**Ttpm – Dacite of Pajarito Mountain, Tshicoma Formation.** Light to medium gray to reddish dacite lavas and associated block and ash flows erupted from Pajarito Mountain. Phenocrysts make up 10–24% of the rock and consist of plagioclase (disequilibrium textures), clinopyroxene, orthopyroxene, and trace hornblende, Fe-Ti oxides, and apatite. Contains crystal clots of clinopyroxene and orthopyroxene. At least 2 major flows are observed in Los Alamos Canyon, overlying Rendija lavas. Brecciated basal horizons typical. Age dates range from  $2.91 \pm 0.06$  to  $3.07 \pm 0.07$  on Pajarito Mountain (WoldeGabriel, pers. communication) with a maximum thickness of ~ 180 meters in map area.

**Ttu – Tshicoma Formation Lavas, Undifferentiated.** This unit, which primarily consists of exposures on the Santa Clara Indian Reservation, represents unmapped territory since access to this region was not allowed. An unnamed center north of Santa Clara Canyon (Smith et al., 1970) is the likely source for  $3.79 \pm 0.17$  to  $4.39 \pm 0.13$  Ma dacite

(WoldeGabriel et al., 2006) exposed in Santa Clara Canyon just north of the quadrangle boundary. Although the majority of the rocks exposed in the canyon are believed to be Tschicoma Formation, older and younger rocks may exist.

**Ttrb – Breccia, white to gray ignimbrite and tephra.** Exposed in a landslide scar in upper Guaje Canyon, west of Guaje Reservoir. Appears to overlie Tti (below). Lower portion includes large lithic fragments of sub-rounded boulders of Rendija Canyon lavas (Ttr). Thin ash and surge beds (< 0.5 meters) occur in the sequence. The upper portion of the deposit appears more as a brecciated lava, containing phenocrysts of plagioclase (some megacrysts), quartz, and lesser biotite and pyroxene. Age most likely comparable to the Rendija Canyon lavas with a maximum exposed thickness of ~ 60 meters.

**Ttrc – rhyodacite of Rendija Canyon, Tschicoma Formation.** . Light to dark gray to red rhyodacitic lavas that form the central part of Sierra de Los Valles. Phenocrysts make up 11-16% of the rock and consist of plagioclase (megacrysts up to 2 cm across), alkali feldspar (both as sanidine and anorthoclase), and quartz (resorbed); subordinate biotite, clinopyroxene, and hornblende; and trace sphene, zircon, and Fe-Ti oxides. Massive, high-aspect ratio flows with associated block and ash flows where oversteepened lava flanks collapsed during flowage. Lavas outcrops can be massive and/or sheeted, and typically exhibit a knobby surface texture that spalls off 1-2 cm-size fragments (enhanced since the Cerro Grande fire). Rendija Canyon lavas north of Guaje Canyon contain moderate amounts of biotite. Maximum thickness is > 350 meters. Age dates range from  $4.95 \pm 0.06$  to  $5.03 \pm 0.02$  (Broxton et al., 2007).

**Tti – Small-volume ignimbrites in upper Guaje Canyon, west of the reservoir.** In ascending order, these tuffs consists of 0.75 m of brown to gray ignimbrite, 13 cm of bedded tuffs, 0.64 m of white ignimbrite, and 0.98 m of light gray to lavender tuff breccia. Phenocrysts of plagioclase and trace amounts of quartz and biotite. Maximum exposed thickness is ~ 2.5 meters. Lower ignimbrite has age date of  $5.32 \pm 0.02$  Ma (WoldeGabriel, pers. communication).

**Keres Group and Santa Fe Group (Miocene).**

**Tbp?** – **Miocene Peralta Tuff Member, Bearhead Rhyolite. (Shown only on cross-section BB’).** Pumice-rich volcanoclastic sediments intercalated with well-bedded tephra. A pumice sample from 508-518 ft. in Well R-2 has a  $^{40}\text{Ar}/^{39}\text{Ar}$  age of  $6.44 \pm 0.46$  Ma. Pumice from 413-423 ft. in R4 gave a poorly constrained  $^{40}\text{Ar}/^{39}\text{Ar}$  age of  $7.6 \pm 1.2$  Ma.

**Tstc?** – **Miocene Chamita Formation, Santa Fe Group. (Shown only on cross-section B-B’).** Well-bedded sandstone with minor gravel at depths of 420 to 494 feet in well R2.

**Tpuv** – **Undivided Miocene Paliza Canyon Formation lava flows and volcanoclastic deposits. (Shown only on cross-sections).**

**Tpa** – **Miocene Keres Group Volcanic Rocks.** Dark gray to red (oxidized) intermediate composition lavas exposed in Santa Clara Canyon, Los Alamos Canyon, and the Pine Springs area. The andesite in Santa Clara Canyon is platy, dark gray, and porphyritic with phenocrysts of plagioclase (Woldegabriel et al., 2006). The  $^{40}\text{Ar}/^{39}\text{Ar}$  age for this andesite is  $7.78 \pm 0.04$  Ma. In Los Alamos Canyon, the porphyritic andesite lava at the reservoir outlet has 20% phenocrysts of plagioclase, clinopyroxene, and orthopyroxene and an  $^{40}\text{Ar}/^{39}\text{Ar}$  age date of  $8.72 \pm 0.05$  Ma (Broxton et al., 2007). This flow also has crystal clots of clinopyroxene, orthopyroxene, and plagioclase. Vesicular facies are common in the Pine Springs area, where four separate outcrops occur, representing two lava types. One appears more dacitic, with larger phenocrysts of plagioclase and lighter color, and one more andesitic, with a dark, fine-grained groundmass with smaller phenocrysts of plagioclase and pyroxene. WoldeGabriel et al. (2006) report an  $^{40}\text{Ar}/^{39}\text{Ar}$  age of  $11.18 \pm 0.13$  Ma on an andesite in the southernmost outcrop at Pine Spring. The three northern outcrops are red (oxidized), but the southernmost outcrop is relatively unaltered. Maximum exposed thickness is ~ 40 meters.

**Tpd** - Outcrop in Guaje Canyon is a crystal-poor lava with conspicuous phenocrysts of sanidine and numerous felty crystals of amphibole, most of which are altered. Sanidine comprises <3% of the whole rock, while amphibole comprises ~3% of the whole rock. Some quartz is present, but whether these are quartz phenocrysts or silicic vug fill is unclear. Small

mafic crystals are also present; these appear to be pyroxenes. A  $^{40}\text{Ar}/^{39}\text{Ar}$  age of  $9.58 \pm 0.13$  Ma was determined for this dacite.

**T1b – Miocene Polvadera Group Volcanic Rocks.** Dark gray to black basalt with olivine and plagioclase phenocrysts correlated with the Lobato Formation.  $^{40}\text{Ar}/^{39}\text{Ar}$  ages of 10.2-13.1 Ma were determined for basalt flows in the Lobato Formation just north of the quadrangle boundary (WoldeGabriel et al., 2006).

## Appendix II

### Clast count of gravels capping hills southeast and east of Guaje Mountain.

1/9/03 by Shari Kelley and Kirt Kempter. Tt = Tschicoma Formation.

#### Top of hill just north of Rendija Canyon above the “poor-man’s” shooting area

Boulders and pebbles; boulders <10 cm)

Clast composition	N	%	
Tt (Caballo dacite)	3	3.6	Total Tt = 24 (28.9%)
Tt (Rendija rhyodacite)	3	3.6	
Undifferentiated Tt	18	21.7	
Flow banded rhyolite	16	19.2	
Obsidian	2	2.4	
Black Tuff	17	20.5	
Pumice (crystal-poor)	1	1.2	
White, fine-grained, felsic	15	18.1	
Mafic lava	2	2.4	
Felsic tuff	1	1.2	
Unidentified	5	6.0	

Total 83

#### Hill to north, just east of Tt outcrops of Guaje Mtn. (0385973 3975340 NAD27)

Boulders and pebbles, boulders <15 cm)

Clast composition	N	%	
Tt (Caballo dacite)			
Tt (Rendija rhyodacite)	No Rendija here		
Undifferentiated Tt	31	44.7	
Flow banded rhyolite	12	16.9	
Obsidian	2	2.8	
Black Tuff	10	14.1	
Pumice (crystal-poor)	2	2.8	
White, fine-grained, felsic	7	9.8	
Mafic lava	0	0.0	
Intermediate lava	1	1.4	
Felsic tuff	0	0.0	
Unidentified	5	8.4	

Total 71

Table 1. Geochemistry of pumice units on Guaje Mountain 7.5-minute quadrangle

<u>Locality</u>	<u>UTM coordinates</u>	<u>Sample</u>	<u>P2O5</u>	<u>SiO2</u>	<u>SO2</u>	<u>TiO2</u>	<u>Al2O3</u>	<u>MgO</u>	<u>CaO</u>	<u>MnO</u>	<u>FeO</u>	<u>Na2O</u>	<u>K2O</u>	<u>F</u>	<u>Cl</u>
El Cajete (?)	13 S 386863	gmp-2-05	0.06	74.38	0.09	0.37	13.39	0.31	1.37	0.05	1.44	3.76	4.67	0.00	0.11
Pueblo Canyon	3971192 (NAD 27)	gmp-2-06	0.04	75.24	0.05	0.29	13.26	0.24	1.13	0.04	1.18	3.54	4.70	0.17	0.13
Pumice above Puye Fm.	13S 387155 3976214 (NAD 27)	gmp-3-01	0.00	76.57	0.02	0.05	12.18	0.00	0.29	0.12	1.41	4.33	4.55	0.23	0.25
N side Guaje Canyon		gmp-3-02	0.01	77.00	0.04	0.06	12.07	0.00	0.26	0.04	1.27	4.13	4.63	0.22	0.28
		gmp-3-03	0.05	77.11	0.01	0.02	12.00	0.00	0.26	0.05	1.32	3.91	4.65	0.36	0.27
		gmp-3-04	0.00	76.97	0.04	0.06	12.14	0.00	0.28	0.07	1.34	3.91	4.75	0.13	0.30
		gmp-3-05	0.04	75.94	0.03	0.08	12.52	0.01	0.28	0.10	1.43	4.38	4.79	0.20	0.21
		gmp-3-06	0.00	76.74	0.03	0.03	12.24	0.01	0.25	0.09	1.26	4.58	4.40	0.13	0.24
		gmp-3-07	0.09	76.72	0.02	0.00	12.21	0.00	0.24	0.07	1.25	4.17	4.65	0.30	0.28
		gmp-3-08	0.03	76.84	0.06	0.05	11.91	0.02	0.26	0.07	1.35	4.15	4.58	0.16	0.51
		gmp-3-09	0.00	76.66	0.00	0.00	12.09	0.00	0.24	0.12	1.30	4.40	4.57	0.39	0.22
		gmp-3-10	0.03	76.74	0.05	0.08	12.13	0.03	0.23	0.10	1.33	4.19	4.65	0.16	0.28
		gmp-3-11	0.03	77.14	0.04	0.03	12.13	0.03	0.28	0.08	1.30	4.17	4.45	0.00	0.32
		gmp-3-12	0.05	76.58	0.00	0.10	12.29	0.00	0.29	0.17	1.23	4.30	4.61	0.09	0.27
		gmp-3-13	0.04	76.53	0.01	0.09	12.29	0.00	0.27	0.08	1.30	4.44	4.67	0.03	0.24
		gmp-3-14	0.01	76.34	0.06	0.01	12.26	0.00	0.32	0.08	1.26	4.43	4.44	0.40	0.39
		gmp-3-15	0.01	76.84	0.06	0.01	12.10	0.00	0.29	0.09	1.18	4.25	4.49	0.27	0.41
		gmp-3-16	0.00	76.24	0.06	0.00	12.10	0.00	0.36	0.13	1.43	4.19	4.65	0.46	0.38
		gmp-3-17	0.00	76.40	0.03	0.02	12.30	0.01	0.30	0.05	1.31	4.30	4.69	0.34	0.25
				<b>gmp-3-average</b>	<b>0.02</b>	<b>76.67</b>	<b>0.03</b>	<b>0.04</b>	<b>12.17</b>	<b>0.01</b>	<b>0.28</b>	<b>0.09</b>	<b>1.31</b>	<b>4.25</b>	<b>4.60</b>
Caballo Peak apartments driveway	13S 382350 3971890 (NAD 27)	gmp-4-01	0.03	77.03	0.00	0.08	12.56	0.03	0.30	0.03	1.02	3.79	4.98	0.00	0.16
		gmp-4-02	0.00	76.86	0.00	0.15	12.56	0.01	0.36	0.03	0.96	3.83	5.04	0.06	0.12
		gmp-4-03	0.00	76.85	0.08	0.06	12.62	0.03	0.36	0.07	0.89	3.77	4.97	0.16	0.14
		gmp-4-04	0.02	76.94	0.02	0.08	12.42	0.02	0.35	0.06	0.99	3.78	5.00	0.16	0.16
		gmp-4-05	0.00	76.87	0.03	0.10	12.32	0.01	0.35	0.04	0.99	3.64	5.28	0.18	0.17
		gmp-4-06	0.00	76.64	0.03	0.14	12.32	0.05	0.34	0.04	0.99	3.88	5.00	0.34	0.22
		gmp-4-07	0.00	77.27	0.03	0.10	12.47	0.04	0.37	0.02	0.98	3.36	5.08	0.00	0.30
		gmp-4-08	0.00	76.63	0.02	0.12	12.67	0.02	0.35	0.08	0.92	3.91	5.00	0.11	0.18
		gmp-4-09	0.00	76.73	0.04	0.07	12.57	0.05	0.36	0.09	0.97	3.63	5.15	0.11	0.23
		gmp-4-10	0.02	76.93	0.03	0.13	12.31	0.03	0.35	0.05	0.92	3.76	5.16	0.20	0.12

gmp-4-11	0.05	76.73	0.00	0.13	12.59	0.02	0.36	0.09	0.93	3.85	5.08	0.04	0.13
gmp-4-12	0.06	76.36	0.03	0.05	12.76	0.07	0.37	0.07	1.05	3.73	5.06	0.14	0.24
gmp-4-13	0.00	77.11	0.09	0.08	12.52	0.04	0.36	0.13	0.94	3.03	5.42	0.13	0.14
gmp-4-14	0.00	76.94	0.00	0.08	12.36	0.02	0.34	0.03	0.98	3.51	5.45	0.00	0.30
gmp-4-15	0.00	76.71	0.00	0.15	12.50	0.03	0.35	0.03	1.01	3.80	5.10	0.20	0.12
gmp-4-16	0.00	76.95	0.00	0.07	12.21	0.02	0.35	0.05	1.01	3.77	5.15	0.25	0.16
gmp-4-17	0.00	77.14	0.03	0.11	12.37	0.01	0.28	0.05	0.89	3.44	5.43	0.05	0.21
gmp-4-18	0.04	76.66	0.00	0.03	12.61	0.04	0.32	0.06	0.91	3.71	5.30	0.12	0.20
gmp-4-19	0.02	77.04	0.00	0.11	12.25	0.04	0.35	0.06	1.02	3.72	5.22	0.02	0.14
gmp-4-20	0.00	76.73	0.01	0.12	12.39	0.01	0.41	0.08	0.91	3.88	4.88	0.41	0.18
gmp-4-21	0.00	76.97	0.00	0.07	12.54	0.04	0.34	0.06	0.88	3.73	5.22	0.00	0.15
gmp-4-22	0.00	76.84	0.00	0.07	12.64	0.00	0.33	0.02	0.86	4.09	4.77	0.23	0.15
gmp-4-23	0.00	77.01	0.03	0.04	12.47	0.02	0.39	0.10	0.89	3.91	4.83	0.16	0.15
gmp-4-24	0.00	76.75	0.03	0.14	12.45	0.02	0.37	0.02	0.99	3.35	5.55	0.14	0.19
gmp-4-25	0.00	76.76	0.04	0.09	12.55	0.04	0.36	0.06	0.90	3.93	4.96	0.15	0.16
<b>gmp-4-average</b>	<b>0.01</b>	<b>76.86</b>	<b>0.02</b>	<b>0.09</b>	<b>12.48</b>	<b>0.03</b>	<b>0.35</b>	<b>0.06</b>	<b>0.95</b>	<b>3.71</b>	<b>5.12</b>	<b>0.13</b>	<b>0.18</b>

Pine Springs	13S 383798	02-gmp-8-01	0.03	72.91	0.03	0.42	14.46	0.57	1.88	0.02	1.97	3.48	3.88	0.23	0.10
dacite of Caballo	3980705	02-gmp-8-02	0.05	73.60	0.01	0.40	14.18	0.45	1.82	0.03	1.72	3.77	3.85	0.00	0.13
Mountain tephra	(NAD 27)	02-gmp-8-03	0.03	72.88	0.02	0.40	14.39	0.46	1.78	0.05	1.84	3.88	3.96	0.21	0.11
		02-gmp-8-04	0.08	72.27	0.06	0.40	14.84	0.55	1.84	0.04	2.03	3.68	3.81	0.19	0.20
		02-gmp-8-05	0.09	72.54	0.05	0.37	15.05	0.54	1.72	0.04	2.11	3.38	3.84	0.12	0.16
		02-gmp-8-06	0.05	73.18	0.03	0.38	14.31	0.50	1.82	0.07	1.81	3.45	4.09	0.12	0.19
		02-gmp-8-07	0.10	72.06	0.00	0.41	15.58	0.20	2.32	0.05	1.07	3.45	4.69	0.05	0.00
		02-gmp-8-08	0.13	71.57	0.00	0.43	15.07	0.81	2.14	0.03	1.30	3.82	4.63	0.07	0.00
		02-gmp-8-09	0.01	72.72	0.04	0.39	14.37	0.45	1.87	0.07	1.68	4.26	3.58	0.22	0.34
		02-gmp-8-11	0.11	73.28	0.00	0.42	14.32	0.44	1.78	0.07	1.66	4.08	3.57	0.20	0.08
		02-gmp-8-12	0.08	73.19	0.04	0.42	14.35	0.44	1.73	0.07	1.76	4.18	3.57	0.11	0.08
		02-gmp-8-13	0.08	73.09	0.00	0.42	14.53	0.48	1.81	0.01	1.68	4.13	3.56	0.12	0.09
		02-gmp-8-16	0.07	73.09	0.00	0.43	14.43	0.45	1.84	0.07	1.87	4.14	3.52	0.00	0.09
		02-gmp-8-17	0.03	73.30	0.05	0.45	14.24	0.41	1.86	0.05	1.81	3.96	3.59	0.02	0.23
		02-gmp-8-18	0.11	72.71	0.03	0.36	14.71	0.51	1.82	0.02	1.84	4.25	3.52	0.02	0.09
		02-gmp-8-20	0.08	73.96	0.00	0.37	14.25	0.45	1.49	0.03	1.58	3.52	4.12	0.00	0.14
		02-gmp-8-21	0.03	74.07	0.00	0.38	13.98	0.40	1.49	0.03	1.62	4.03	3.54	0.30	0.14
		02-gmp-8-23	0.07	72.79	0.01	0.46	14.51	0.53	1.88	0.03	1.83	4.28	3.46	0.07	0.08
		02-gmp-8-24	0.09	73.12	0.02	0.43	14.46	0.43	1.74	0.03	1.80	4.23	3.50	0.03	0.10
		02-gmp-8-25	0.02	73.50	0.04	0.40	14.23	0.46	1.69	0.04	1.73	4.00	3.67	0.11	0.10

			<b>02-gmp-8-mean</b>	<b>0.07</b>	<b>####</b>	<b>###</b>	<b>###</b>	<b>14.51</b>	<b>0.48</b>	<b>###</b>	<b>0.04</b>	<b>###</b>	<b>3.90</b>	<b>###</b>	<b>###</b>	<b>###</b>
			st. dev.	0.03	0.60	0.02	0.03	0.37	0.11	0.18	0.02	0.23	0.31	0.36	0.09	0.08
Pine Springs	13S 384456	antler hill-01	0.00	77.00	0.00	0.09	12.18	0.02	0.35	0.02	0.83	3.07	5.90	0.39	0.13	
Antler Hill	3979221	antler hill-03	0.00	77.16	0.00	0.12	12.43	0.04	0.38	0.02	0.73	3.46	5.50	0.01	0.15	
	(NAD 27)	antler hill-04	0.00	77.56	0.00	0.12	12.36	0.02	0.39	0.04	0.81	3.03	5.53	0.00	0.15	
		antler hill-05	0.02	76.90	0.01	0.10	12.50	0.03	0.34	0.06	0.83	3.23	5.73	0.11	0.13	
		antler hill-06	0.00	77.35	0.01	0.08	12.37	0.03	0.45	0.05	0.77	3.84	4.72	0.18	0.14	
		antler hill-07	0.00	76.74	0.00	0.11	12.62	0.05	0.36	0.05	0.76	3.68	5.30	0.17	0.14	
		antler hill-08	0.00	77.18	0.00	0.12	12.31	0.03	0.39	0.07	0.84	3.24	5.50	0.16	0.17	
		antler hill-10	0.00	77.14	0.00	0.09	12.53	0.05	0.34	0.06	0.74	3.88	4.93	0.11	0.12	
		antler hill-11	0.02	76.97	0.02	0.09	12.34	0.03	0.39	0.06	0.80	3.34	5.55	0.23	0.16	
		antler hill-12	0.05	76.90	0.00	0.17	12.43	0.04	0.37	0.06	0.85	3.85	5.05	0.10	0.12	
		antler hill-13	0.10	77.11	0.02	0.04	12.43	0.04	0.37	0.05	0.74	3.50	5.48	0.00	0.13	
		antler hill-14	0.02	77.46	0.00	0.05	12.29	0.02	0.36	0.04	0.73	3.28	5.61	0.00	0.15	
		antler hill-15	0.02	77.01	0.01	0.10	12.45	0.04	0.40	0.08	0.75	3.44	5.49	0.06	0.15	
		antler hill-16	0.00	77.46	0.03	0.02	12.46	0.03	0.36	0.08	0.75	3.69	4.93	0.05	0.14	
		antler hill-17	0.00	77.15	0.02	0.13	12.41	0.05	0.42	0.02	0.86	2.93	5.78	0.00	0.22	
		antler hill-18	0.00	77.43	0.01	0.09	12.39	0.02	0.41	0.03	0.81	2.95	5.62	0.10	0.14	
		antler hill-19	0.00	77.01	0.01	0.11	12.42	0.05	0.33	0.08	0.79	3.38	5.36	0.29	0.15	
		antler hill-20	0.00	76.91	0.01	0.15	12.28	0.02	0.44	0.05	0.77	3.19	5.77	0.22	0.19	
		antler hill-21	0.00	77.15	0.01	0.15	12.29	0.04	0.37	0.04	0.87	3.31	5.53	0.06	0.19	
		antler hill-22	0.00	76.92	0.01	0.17	12.50	0.04	0.36	0.07	0.75	3.90	5.06	0.06	0.15	
		antler hill-23	0.00	77.47	0.02	0.12	12.34	0.03	0.36	0.07	0.77	3.79	4.86	0.04	0.13	
		antler hill-24	0.05	76.99	0.04	0.08	12.46	0.05	0.37	0.10	0.76	3.37	5.46	0.06	0.19	
		antler hill-25	0.03	77.00	0.02	0.02	12.52	0.05	0.42	0.06	0.84	3.53	5.30	0.09	0.11	
		<b>antler hill-mean</b>	<b>0.01</b>	<b>77.13</b>	<b>0.01</b>	<b>0.10</b>	<b>12.40</b>	<b>0.04</b>	<b>0.38</b>	<b>0.06</b>	<b>0.79</b>	<b>3.43</b>	<b>5.39</b>	<b>0.11</b>	<b>0.15</b>	

Normalized to 100%

Data obtained by Nelia Dunbar using the electron microprobe at the New Mexico Bureau of Geology and Mineral Resources

Table 2. Geochemical data for samples collected as part of this study.

**XRF Analyses of unknowns at 9:1 dilution by Group EES-6, LANL**

<b>Sample Number</b>	<b>DEB9/05-1</b>	<b>(same sample as 05GM05 on next page)</b>
		error
SiO2 avg %	66.00	0.87
TiO2 avg %	0.481	0.013
Al2O3 avg %	16.15	0.28
Fe2O3T avg %	3.63	0.05
MnO avg %	0.055	0.007
MgO avg %	1.12	0.05
CaO avg %	3.98	0.08
Na2O avg %	4.63	0.10
K2O avg %	2.31	0.05
P2O5 avg %	0.214	0.009
LOI %	0.32	
Total Maj avg %	98.58	
V avg ppm	70.2	15.2
Cr avg ppm	12.1	9.9
Ni avg ppm	9.1	5.6
Zn avg ppm	72.9	11.5
Rb avg ppm	30.6	4.6
Sr avg ppm	956.7	38.2
Y avg ppm	-8.0	
Zr avg ppm	168.4	19.3
Nb avg ppm	-7.6	
Ba avg ppm	1233.0	41.3
Total Trace avg %	0.30	
Total avg %	98.88	
Total + LOI	99.20	

\*Trace totals as oxides. Negative values indicate '<', except for LOI. Negative LOI values, which indicate weight gain during ignition, are used in calculating flux to sample ratios, but are not added to the total. Analytical uncertainties are 2 sigma, in same units as analyses.

<b>Field #</b>	03-29-02-2	05GM05
<b>Description</b>	Ignimbrite	Guaje Canyon
<b>Location</b>	13S 380521	383544
<b>(NAD 27)</b>	3977202	3977243
<b>comp</b>	<b>rhyolite</b>	<b>dacite</b>
<b>rSiO2%</b>	75.6	66.0
<b>rAl2O3%</b>	12.8	16.2
<b>rFeTO3%</b>	1.66	3.62
<b>rMgO%</b>	0.30	1.64
<b>rCaO%</b>	1.01	3.98
<b>rNa2O%</b>	2.44	4.27
<b>rK2O%</b>	5.05	2.24
<b>rTiO2%</b>	0.10	0.48
<b>rP2O5%</b>	0.09	0.30
<b>rMnO%</b>	0.09	0.06
<b>LOI%</b>	7.25	0.26
<b>Total</b>	99.20	98.81
<b>Lab #</b>	C-268757	C-268756
<b>Fe%</b>	1.11	2.62
<b>Ca%</b>	0.89	3.19
<b>Na%</b>	1.91	3.54
<b>K %</b>	3.79	1.90
<b>Rb ppm</b>	418	27.2
<b>Sr ppm</b>	318	995
<b>Cs ppm</b>	15.7	0.30
<b>Ba ppm</b>	236	1260
<b>Th ppm</b>	26.1	6.51
<b>U ppm</b>	7.35	2.31
<b>La ppm</b>	55.7	37.3
<b>Ce ppm</b>	100	56.7
<b>Nd ppm</b>	60.2	21.1
<b>Sm ppm</b>	15.3	3.57
<b>Eu ppm</b>	0.27	1.02
<b>Gd ppm</b>	16.5	2.86
<b>Tb ppm</b>	2.50	0.36
<b>Ho ppm</b>	3.31	0.41
<b>Tm ppm</b>	1.37	0.16
<b>Yb ppm</b>	8.34	0.97
<b>Lu ppm</b>	1.170	0.148
<b>Zr ppm</b>	270	129
<b>Hf ppm</b>	9.65	3.71

Ta ppm	7.83	1.08
W ppm	3.86	1.63
Sc ppm	2.08	6.50
Cr ppm	2.0	21.5
Co ppm	0.85	9.89
Ni ppm	6.27	16.4
Zn ppm	104	52.8
As ppm	1.82	0.33
Sb ppm	0.47	0.06
Au ppb	3.4	<3.2

	C- 268757	C- 268756
La	179.10	119.94
Ce	123.00	69.74
Pr		
Nd	99.67	34.93
Sm	78.06	18.21
Eu	3.61	13.78
Gd	63.46	11.00
Tb	53.19	7.74
Dy		
Ho	46.10	5.71
Er		
Tm	42.02	4.88
Yb	39.71	4.63
Lu	36.22	4.58

Analyzed by the U. S. Geological Survey. Thanks to David Sawyer for his help in obtaining these data.

**Table 1.  $^{40}\text{Ar}/^{39}\text{Ar}$  analytical data.**

ID	Temp (°C)	$^{40}\text{Ar}/^{39}\text{Ar}$	$^{37}\text{Ar}/^{39}\text{Ar}$	$^{36}\text{Ar}/^{39}\text{Ar}$ ( $\times 10^{-3}$ )	$^{39}\text{Ar}_k$ ( $\times 10^{-15}$ mol)	K/Ca	$^{40}\text{Ar}^*$ (%)	$^{39}\text{Ar}$ (%)	Age (Ma)	$\pm 1\sigma$ (Ma)	
<b>05GM05</b> , Groundmass Concentrate, 77 mg, J=0.0007142±0.10%, D=1.003±0.001, NM-191H, Lab#=55886-01											
Xi A	625	1856.8	-0.0169	6291.3	0.115	-	-0.1	0.1	-3	16	
B	750	9.654	0.5357	7.660	21.9	0.95	77.0	11.0	9.558	0.050	
C	850	8.321	0.4603	1.968	23.0	1.1	93.5	22.5	9.997	0.032	
D	950	7.825	0.5461	1.615	104.9	0.93	94.5	74.9	9.505	0.017	
E	1050	8.874	0.9145	5.447	32.7	0.56	82.7	91.2	9.439	0.032	
F	1125	16.67	1.422	32.16	9.90	0.36	43.7	96.2	9.37	0.12	
X G	1200	37.14	2.843	104.7	4.22	0.18	17.3	98.3	8.29	0.30	
X H	1300	86.12	9.794	265.3	1.18	0.052	9.9	98.9	11.0	1.0	
Xi I	1700	88.92	7.355	277.3	2.27	0.069	8.5	100.0	9.79	0.88	
<b>Integrated age <math>\pm 2\sigma</math></b>			n=9		200.2	0.62	K <sub>2</sub> O=1.40%		9.53	0.08	
<b>Plateau <math>\pm 2\sigma</math></b>			steps B-F	n=5	MSWD=53.3	192.4	0.86 $\pm$ 0.62		96.1	9.58	0.19
<b>Isochron<math>\pm 2\sigma</math></b>			steps B-H	n=7	MSWD=45.3		$^{40}\text{Ar}/^{36}\text{Ar}= 291\pm 20$		9.60	0.23	
<b>05GM05</b> , Plagioclase, 41.22 mg, J=0.0007157±0.07%, D=1.003±0.001, NM-191H, Lab#=55887-01											
Xi A	650	535.7	8.263	1781.9	0.033	0.062	1.8	0.1	13	15	
B	775	13.93	7.359	25.74	0.721	0.069	49.8	2.7	8.98	0.44	
C	850	9.206	7.428	10.07	0.648	0.069	74.4	5.1	8.86	0.57	
D	925	8.557	7.582	6.464	2.15	0.067	85.0	13.0	9.42	0.23	
E	1000	8.072	7.798	4.487	3.30	0.065	91.6	25.0	9.57	0.15	
F	1100	7.832	7.747	3.709	5.31	0.066	94.2	44.4	9.55	0.10	
i G	1175	8.111	7.869	4.324	5.22	0.065	92.3	63.4	9.691	0.098	
Xi H	1250	8.513	8.099	3.703	3.83	0.063	95.0	77.4	10.47	0.13	
Xi I	1350	11.92	8.388	7.071	2.77	0.061	88.3	87.5	13.62	0.18	
Xi J	1450	14.76	7.619	14.22	1.24	0.067	75.8	92.0	14.46	0.39	
Xi K	1675	12.80	8.513	14.49	2.19	0.060	72.1	100.0	11.94	0.23	
<b>Integrated age <math>\pm 2\sigma</math></b>			n=11		27.4	0.064	K <sub>2</sub> O=0.36%		10.46	0.14	
<b>Plateau <math>\pm 2\sigma</math></b>			steps B-G	n=6	MSWD=1.1	17.4	0.066 $\pm$ 0.004		63.3	9.58	0.13
<b>Isochron<math>\pm 2\sigma</math></b>			steps B-F	n=5	MSWD=0.4		$^{40}\text{Ar}/^{36}\text{Ar}= 273\pm 28$		9.60	0.18	
<b>Notes:</b>											
Isotopic ratios corrected for blank, radioactive decay, and mass discrimination, not corrected for interfering reactions.											
Errors quoted for individual analyses include analytical error only, without interfering reaction or J uncertainties.											
Integrated age calculated by summing isotopic measurements of all steps.											
Integrated age error calculated by quadratically combining errors of isotopic measurements of all steps.											
Plateau age is inverse-variance-weighted mean of selected steps.											
Plateau age error is inverse-variance-weighted mean error (Taylor, 1982) times root MSWD where MSWD>1.											
Plateau error is weighted error of Taylor (1982).											
Decay constants and isotopic abundances after Steiger and Jäger (1977).											
X symbol preceding sample ID denotes analyses excluded from plateau age calculations.											
i symbol preceding sample ID denotes analyses excluded from inverse isochron age calculations.											
Weight percent K <sub>2</sub> O calculated from $^{39}\text{Ar}$ signal, sample weight, and instrument sensitivity.											
Ages calculated relative to FC-2 Fish Canyon Tuff sanidine interlaboratory standard at 28.02 Ma											
Decay Constant (LambdaK (total)) = 5.543e-10/a											
Correction factors:											
$(^{39}\text{Ar}/^{37}\text{Ar})_{\text{Ca}} = 0.0007 \pm 5\text{e-}05$											
$(^{36}\text{Ar}/^{37}\text{Ar})_{\text{Ca}} = 0.00028 \pm 1\text{e-}05$											
$(^{38}\text{Ar}/^{39}\text{Ar})_k = 0.013$											
$(^{40}\text{Ar}/^{39}\text{Ar})_k = 0 \pm 0.0004$											

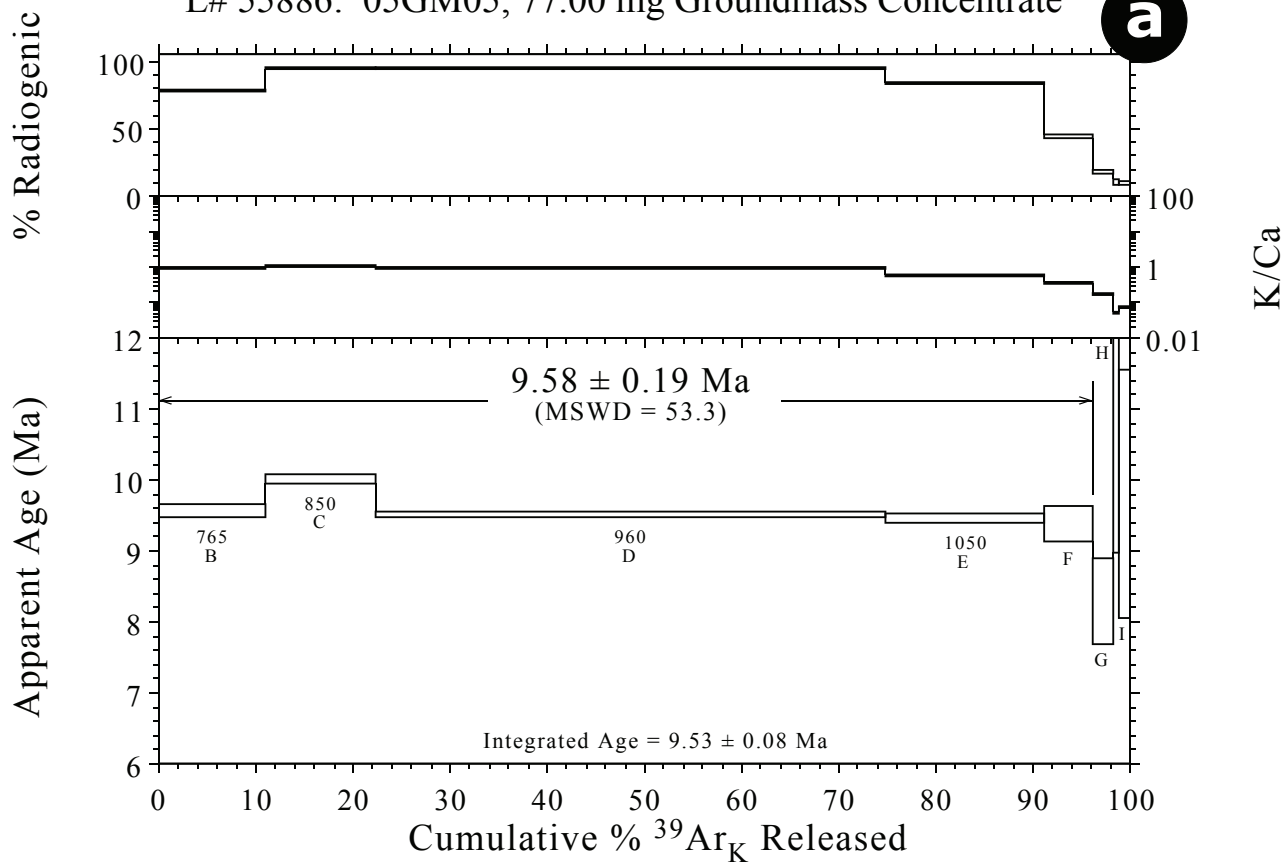
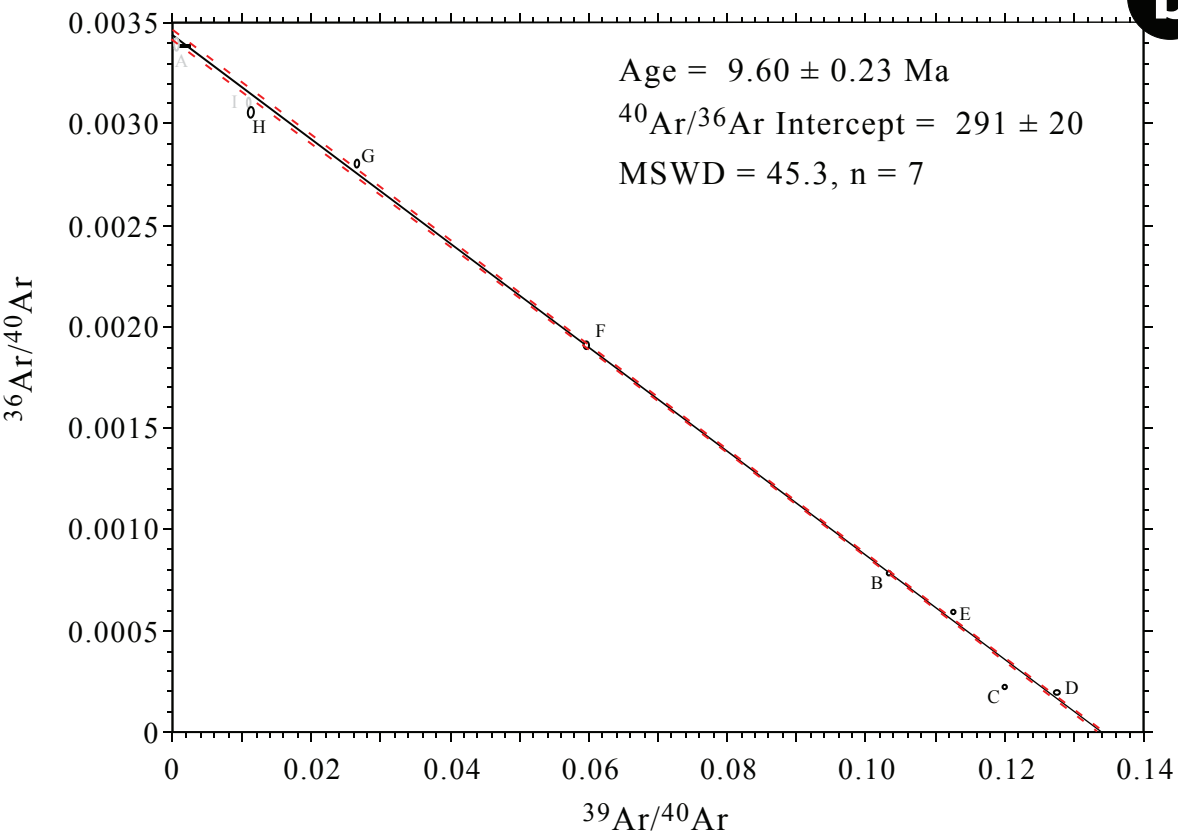
**a****b**

Figure XX. Age spectrum (2a) and isochron (2b) for the 05GM05 groundmass concentrate sample. All errors quoted at two sigma.

L# 55887: 05GM05, 41.22 mg Plagioclase

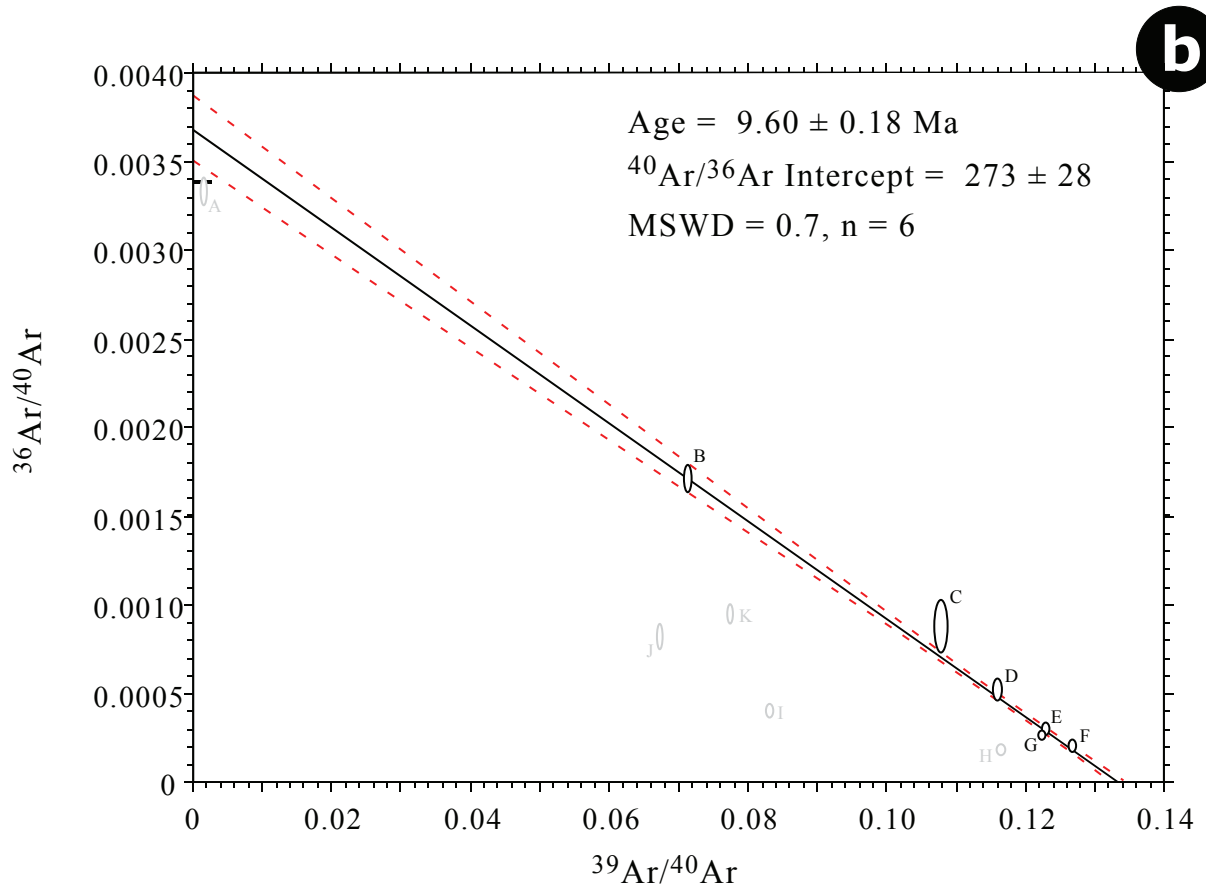
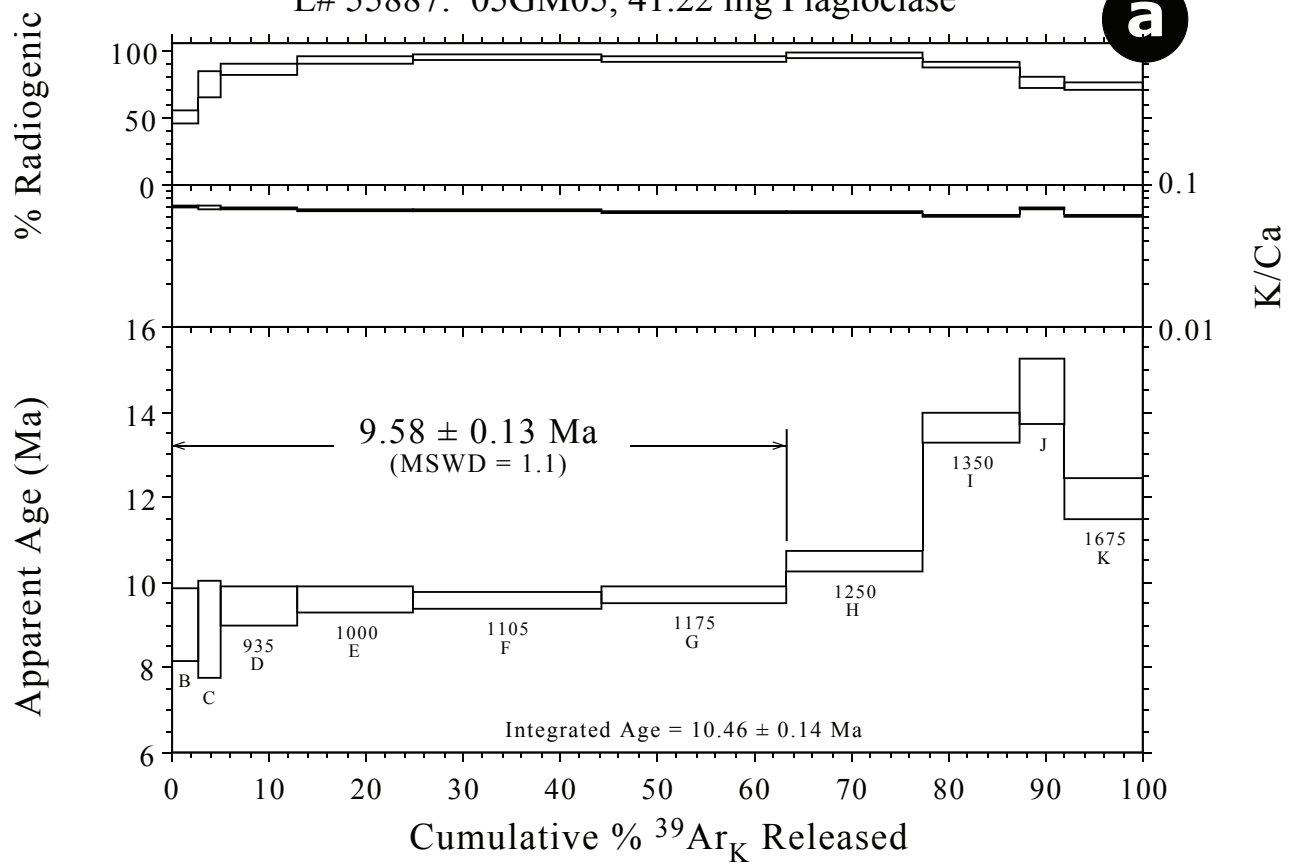


Figure XX. Age spectrum (2a) and isochron (2b) for the 05GM05 plagioclase sample. All errors quoted at two sigma.